603059

DOPPLER ANTENNA INVESTIGATION
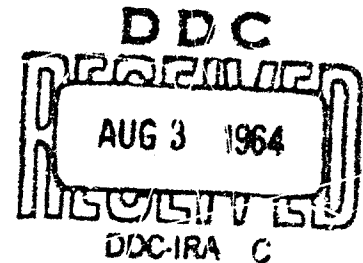
*73 p $Book
$0.75 mf*

TECHNICAL DOCUMENT REPORT
NO. AL-TDR-64-162

July 1964

AF Avionics Laboratory
Research and Technology Division
Air Force Systems Command
Wright-Patterson Air Force Base, Ohio

Project No. 3181, Task No. 318102

Contract AF 04(695)-250

DDC

AUG 3 1964

DDC-IRA C

FOREWORD

This report was prepared by Hughes Aircraft Company,
Culver City, California, on Air Force Contract
AF 04(695)-250, "Doppler Antenna Investigation." The
work was originally administered under the direction of
Space Systems Division. Captain Hollis O. Hall was
Project Engineer. It was subsequently transferred to
the Navigation and Guidance Division of the Air Force
Avionics Laboratory. Mr. Donald A. Guidice, and sub-
sequently, Mr. William Harmon were Project Engineers
for the Laboratory.

Dr. A. T. Villeneuve of the Antenna Department, Hughes
Aircraft Company, was Project Engineer for the program.

The following people have contributed to the program:
F. G. Terrio, W. H. Kummer, C. H. Nonemaker, Jr.,
L. E. Gates, Jr., P. M. Winslow, W. H. Wheeler,
A. A. Miele, W. E. Lent, J. H. Holley, S. Robelotto,
W. E. McKee. F. G. Hup coordinated activities between
the Antenna Department and the Materials Technology
Department.

This report is the final report and it concludes the work
on Contract No. AF 04(695)-250. The Contractor's
report number is P64-15.

ABSTRACT

This report presents the results of a study dealing with the effects of factors such as high temperature and vehicle maneuvers on a rectangular flat plate slot array antenna for lift-reentry vehicles. Specifically, the study consisted of two parts. The first part dealt with an investigation of slot closure techniques which will preserve the electrical performance of the antenna under severe environmental conditions. This consisted of a materials study to determine suitable metals and dielectric materials which have compatible thermodynamic characteristics up to temperatures of 2500°F. When suitable materials had been determined, a number of dielectric to metal bonding techniques were investigated experimentally. The most successful of these bonding techniques was then investigated to determine the electrical properties of the configuration.

As a result of the slot closure study several slots were fabricated in molybdenum plates. These were closed with mullite and electron beam welded to the end of a section of molybdenum X-band guide. The guide itself was electron beam welded from sheet molybdenum. The guide and window together showed insertion losses of 0.35 to 0.45 db at resonance when tested under ambient temperature conditions. High temperature electrical measurements were not performed in this phase of the program.

The second part of the study consisted of an investigation of the problem of beam stablization in the presence of vehicle pitch, roll and yaw maneuvers. Two aspects of the problem were considered. First, the regions within which beam pointing control is required were determined by applying various combinations of pitch and roll to the vehicle carrying the antenna. Since it was anticipated that yaw would be small, it was not considered in numerical calculations. Second, for the type of antenna being considered, the region of possible beam positions was investigated. Devices and techniques for accomplishing the beam positioning were also considered. The high temperatures of the antenna and components ruled out the use of most conventional phase shifting devices.

The results of the beam stabilization studies indicate that for the types of stabilization considered for the flat plate antenna developed under Contract AF 33(616)-10672, the necessary beam positions cannot be obtained with a flush mounted array due to vehicle attitudes during reentry. However, if the array were set so as to be level when the vehicle had its normal attitude, then most of the desired angles could be covered.

Publication of this technical documentary report does not constitute Air Force approval of the findings or conclusions of the report. It is published only for the exchange and stimulation of ideas.

CONTENTS

ILLUSTRATIONS

INTRODUCTION

An object or vehicle traveling at high speeds through the earth's atmosphere experiences heating due to its interaction with the atmosphere. That such heating can be severe is evidenced by the fact that only the largest of the many meteors entering the earth's atmosphere ever reach the ground. The remainder completely burn up in transit through the atmosphere.

The heating in such an environment is normally specified in terms of a heat load - Btu/(hr) (sq ft) — which, for a given vehicle and trajectory, will vary with time and with location on the vehicle surface. The heat transferred to the vehicle surface from the air is accounted for by a rise in surface temperature (heat capacity), conduction into the vehicle, radiation of heat from the hot surface back into space, and evaporation of the surface (ablation).

Generally speaking, with these types of vehicles, as the heat is supplied to the vehicle surface something must be done to dispose of it. Cooling by conducting the heat into the vehicle is not normally acceptable because of the large total amount of heat involved. Therefore, the surface temperature can be expected to rise to high values.

The maximum heat loading encountered by a vehicle depends on the vehicle's size, shape, and trajectory. Roughly, the tradeoff on trajectories is, on one extreme, a rapid reentry lasting a short time with high skin temperatures and, on the other extreme, a slow reentry lasting a long time, as in the case of lift-reentry vehicles, with lower, but still high, temperatures. However, in the latter case the total heat transferred to the vehicle is many times greater than in the former, posing a greater problem as far as keeping the interior cool.

This study is concerned with the problems of slot closure and beam scanning associated with a flat flush-mounted slot array suitable for use as a doppler navigation antenna on a lift type reentry vehicle. Since the array is mounted on the surface of a vehicle passing through the atmosphere at high speeds, the array must withstand severe temperature variations with surface temperatures up to 2500° F. The

primary reason for closing the slots is to prevent erosion of the slot edges by the high speed hot air stream. The reason for investigating beam scanning techniques is to compensate for vehicle motion as it maneuvers during, and subsequent to reentry.

To date this class of vehicles has had only simple antennas (essentially omnidirectional as compared to narrow beam antennas) operating at these temperatures.

There are two basic ways to place a slot array type antenna on a hot vehicle skin. The conceptually simpler of the two is to place the slots on the vehicle surface and to close them with a suitable window material. In this case the antenna operates at skin temperature. The other solution is to recess the antenna into the cooler interior of the vehicle and replace the vehicle skin over the antenna with a window or radome which also serves as a thermal insulator—a so called thermal gradient antenna. The former approach, which was specified for this study, involves advancing the state-of-the-art both in the construction of the array and also in the scanning of a beam from it.

Studies and development work on lift-reentry vehicles have established that design problems associated with large, flush-mounted antennas for such vehicles will be severe. As examples, beam deflection due to warping of the antenna under the influence of thermal gradients, and changes in dielectric coefficients and waveguide transmission characteristics under high temperatures have been experienced. In addition, maintenance of the "reentry corridor" requires changes in vehicle attitude with resulting beam position changes and heat load pattern changes.

This report presents the results of a study dealing with the effects of some of these factors on a rectangular flat plate slot array antenna similar to that being developed concurrently on Contract AF 33(616)-10672. Specifically, the study consisted of two parts. The first part dealt with an investigation of slot closure techniques which will preserve the electrical performance of the antenna under severe environmental conditions. This consisted of a materials study to determine suitable metals and dielectric materials which have compatible thermodynamic

characteristics up to temperatures of 2500°F. When suitable materials had been determined, a number of dielectric to metal bonding techniques were investigated experimentally. The most successful of these bonding techniques was then investigated to determine the electrical properties of the configuration.

As a result of the slot closure study several slots were fabricated in molybdenum plates. These were closed with mullite and electron beam welded to the end of a section of molybdenum X-band guide. The guide itself was electron beam welded from sheet molybdenum. The guide and window together showed insertion losses of 0.35 to 0.45 db at resonance when tested under ambient temperature conditions. Lack of time prevented taking of high temperature electrical measurements.

The second part of the study consisted of an investigation of the problem of beam stabilization in the presence of vehicle pitch, roll and yaw maneuvers. Two aspects of the problem were considered. First, the regions within which beam pointing control is required were determined by applying various combinations of pitch and roll to the vehicle carrying the antenna. Since it was anticipated that yaw would be small it was not considered in numerical calculations. Second, for the type of antenna being considered, the region of possible beam positions was investigated. Devices and techniques for accomplishing the beam positioning were also considered. The high temperatures of the antenna and components ruled out the use of most conventional phase shifting devices.

The results of the beam stabilization studies indicate that for the types of stabilization considered for the flat plate antenna developed under Contract AF 33(616)-10672, the necessary beam positions cannot be obtained with a flush mounted array due to vehicle attitudes during reentry. However, if the array could be set so that it were level when the vehicle had its normal attitude, then most of the desired angles could be covered.

The details of the studies are presented in the following sections of the report.

3

TECHNICAL DISCUSSION

One of the purposes of this study is to investigate techniques for closure of slots in flat plate antennas of the type being developed concurrently on Contract AF 33(616)-10672. These closures are to be such that antenna performance is maintained at temperatures up to 2500°F.* The slot closures are intended to protect the antenna slots from erosion by preventing contact of the slot openings with the flow of high velocity, high temperature air over the antenna. In such an investigation one of the first considerations must be the electrical aspects of the covering configuration and its effect upon antenna performance. The conclusions of such a study are, of course, influenced by the methods available for fabricating and bonding any cover to the array.

DESCRIPTION OF THE ARRAY

The type of rectangular array being considered consists of a number of parallel linear arrays. Each linear array is of a leaky wave type and consists of a waveguide with slots closely spaced along its length in the radiating wall. The coupling of radiation out of the guide depends on the slot lengths and on their spacing relative to the guide wavelength. The presence of a dielectric cover material near the slots will affect this coupling and must be considered in array design.

EFFECTS OF DIELECTRIC COVERING

Unfortunately, the relative permittivity of dielectric materials varies over the temperature range of interest and the characteristics of the antenna become temperature sensitive because of this effect.

---

*Studies of techniques capable of providing closed slot antennas for temperatures up to 2000°F are also being conducted at Cornell Aeronautical Laboratory on Contract AF 33(657)-11100.

Because of this it appears desirable to have a covering which does not extend into the slots themselves where the fields are strong and the interaction of the fields and dielectric is greatest. In addition, dielectric materials with large relative permitivities increase the frequency sensitivity of the slots, making the covered slot couplings more frequency dependent than those for uncovered slots. This second consideration implies that relative permitivities close to unity are desirable as covering materials. Other investigators have studied the possibility of using ablative materials for covering the slots.[1] Design procedures were developed for arrays using such coverings. It was found that covers which exceeded a certain minimum thickness did not change slot characteristics significantly as the dielectric thickness increased from this minimum. Therefore, as the material ablated on reentry, the array characteristics would be maintained until the material reached the minimum thickness.

For the present application, however, rather extended periods at high temperatures as well as a possibility of repeated missions are contemplated, thereby ruling out the use of ablative techniques.

From these considerations it appears desirable to look for a technique which can place a thin sheet of low permitivity, high temperature, dielectric material directly over the slotted array surface without allowing the material to extend into the slots.

With such an ideal configuration in mind some experiments were conducted (at room temperature) to obtain information on the effects of the cover on a slotted plate radiator covered with dielectric sheets. The test configuration consisted of square waveguide (0.8 x 0.8 inches, inside dimensions) with centered longitudinal slots in one side wall. This is similar to the longitudinal slot configurations used in the doppler velocity sensor antenna already referred to. The aperture distributions of such an array may be measured in terms of a leakage attenuation per unit length which is due to the radiation from the slots. If the slots are covered with a dielectric, the dielectric tends to alter the electrical characteristics of the slot. Figures 1a through 1d give the results of
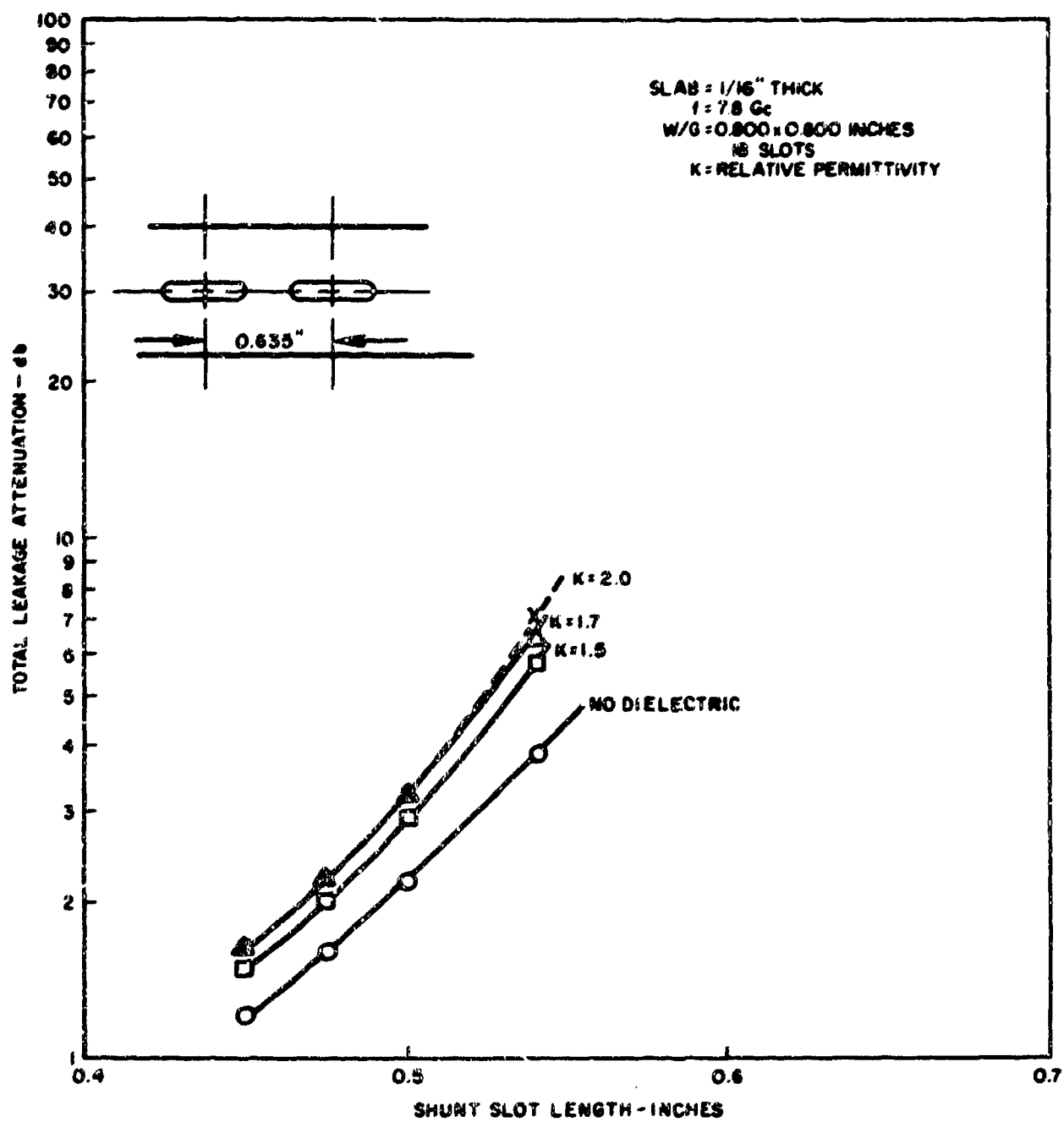
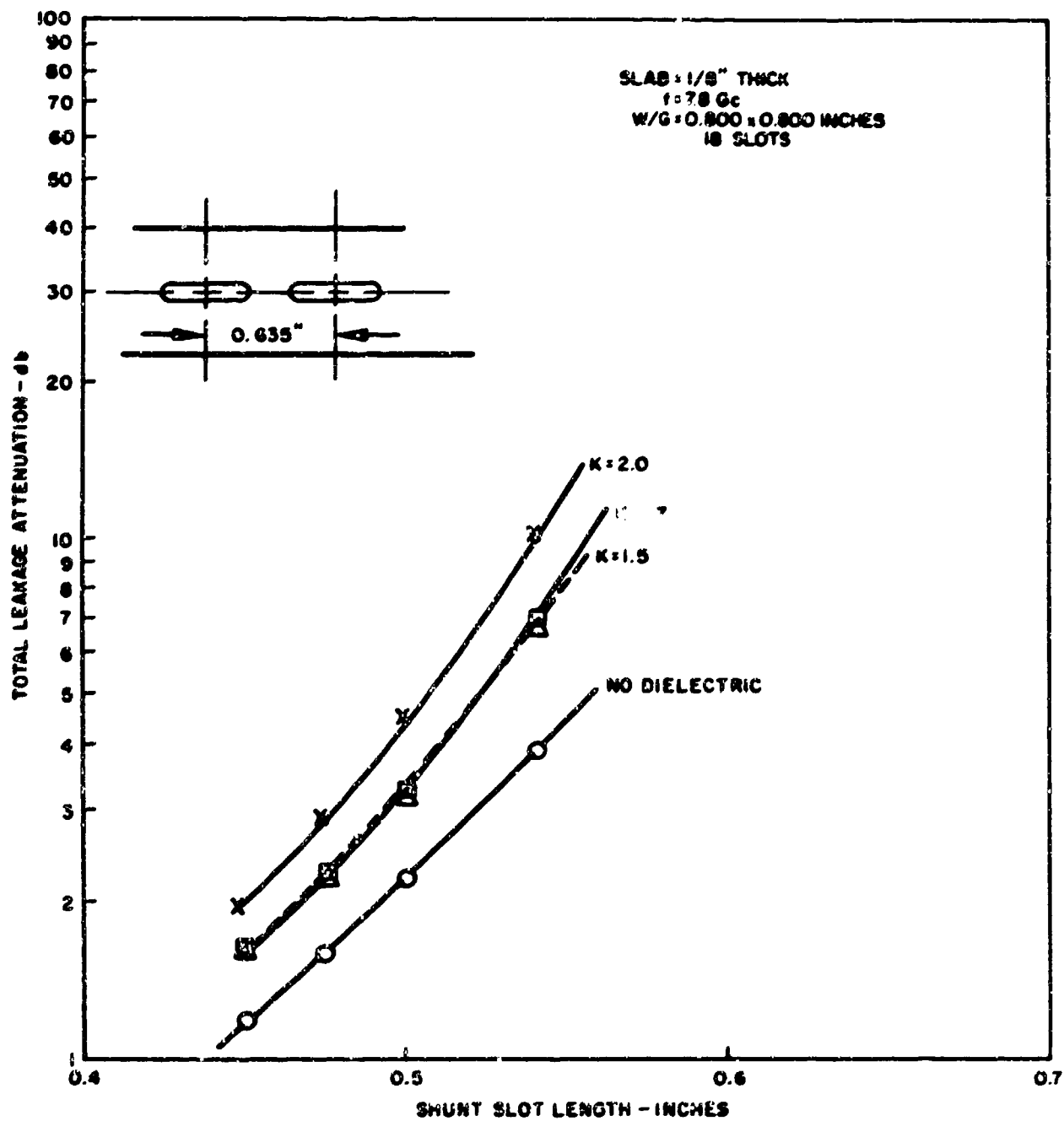Figure 1a.   Leakage attenuation of slab covered slot array.

7

Figure 1b. Leakage attenuation of slab covered slot array.
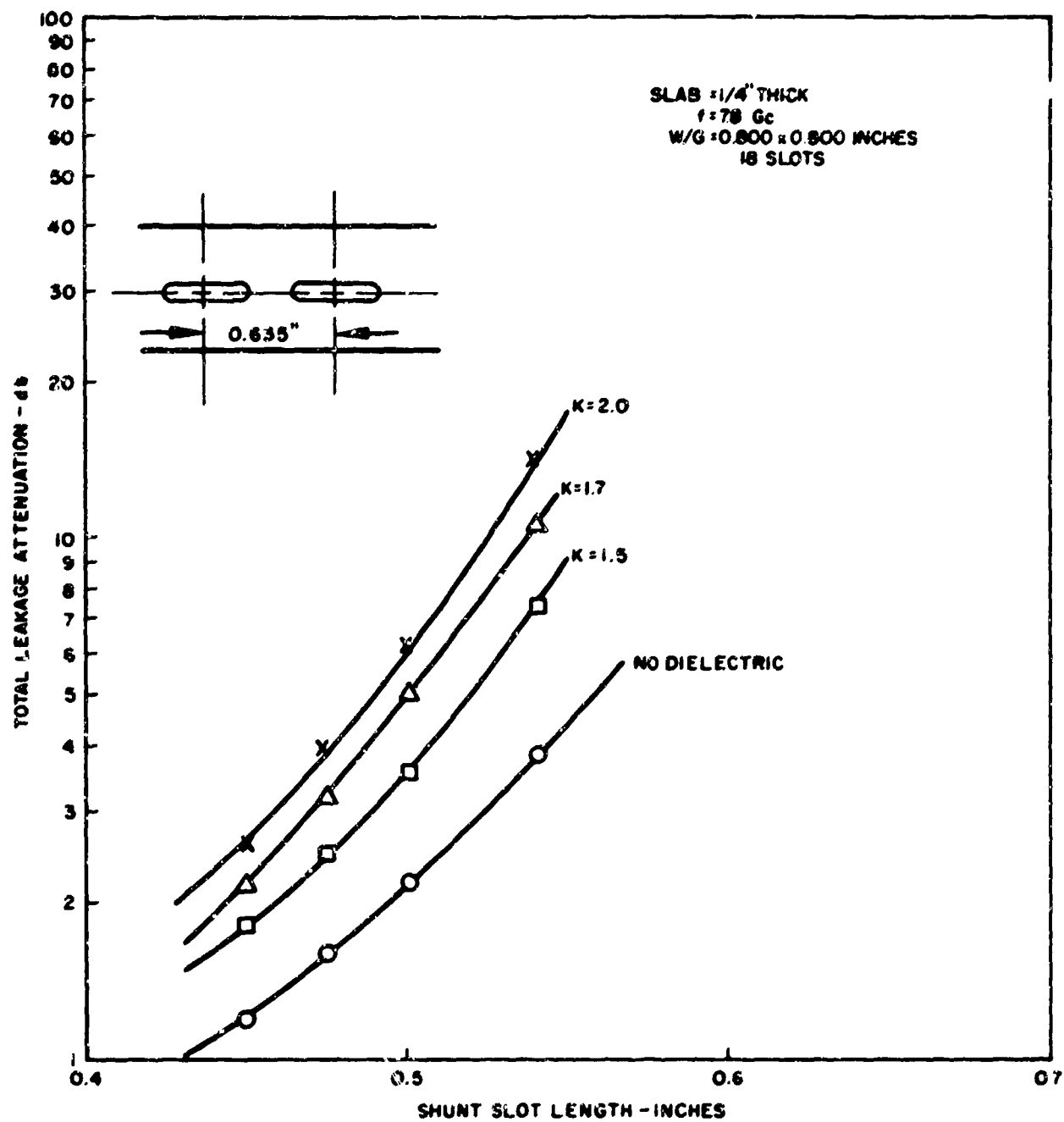
Figure 1c.   Leakage attenuation of slab covered slot array.

9
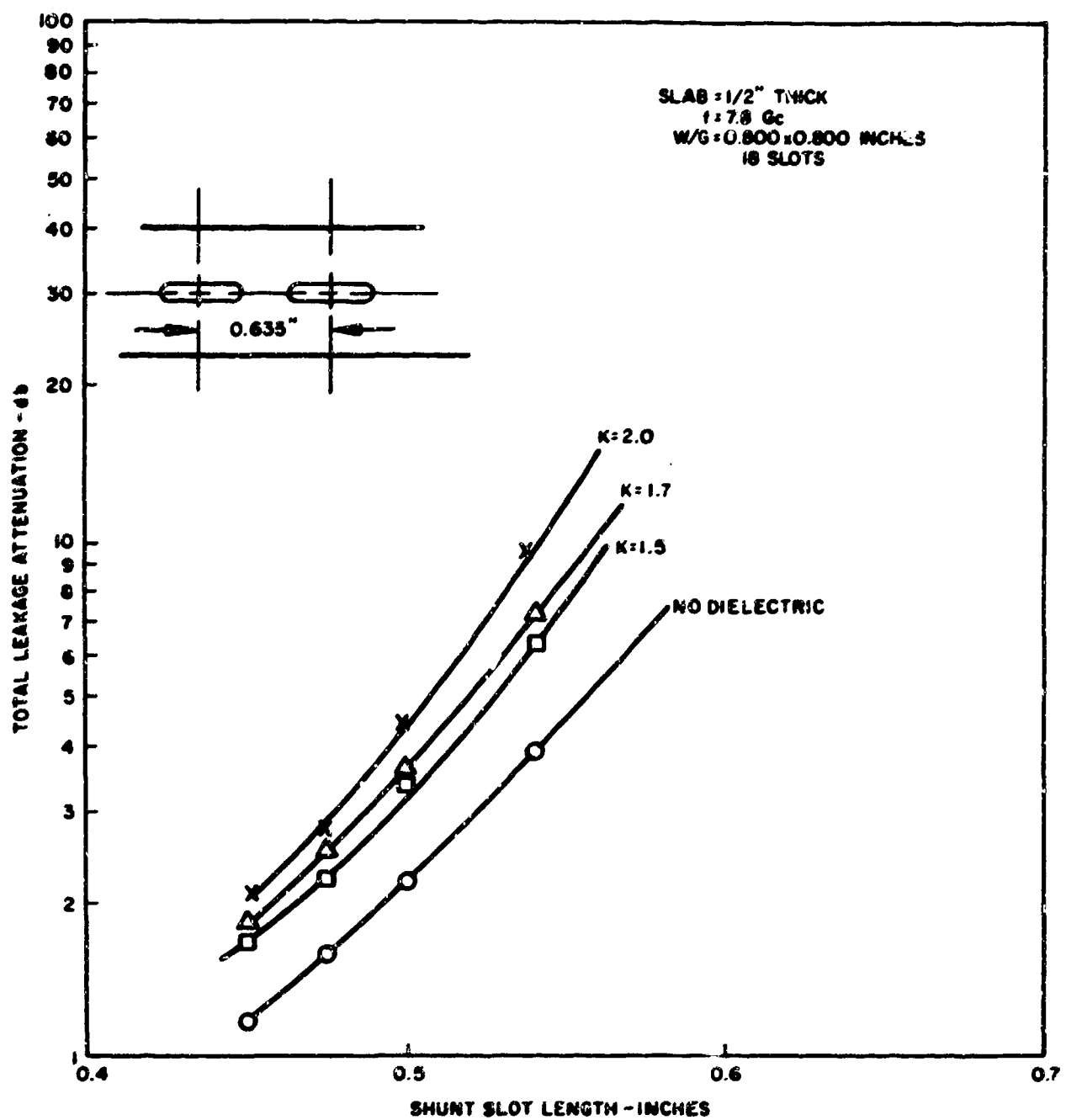
Figure 1d.   Leakage attenuation of slab covered slot array.

measurements of the coupling dependence of short slots in square
waveguide on the thickness and dielectric constant of the cover slab.
The frequency, number of slots, and cover thickness were held constant
as the length of the slots was varied for a number of different dielectric
covers. The total leakage attenuation of the slotted section was measured
in db (each section is about 11.5 inches long). Each graph is for a
different thickness of dielectric cover—1/16, 1/8, 1/4 and 1/2 inch.
It is evident that even these relatively low dielectric constants have a
significant effect on the aperture distribution of such an array. It
should be pointed out that for these measurements the slabs were not
bonded to the guide. The measurements were, therefore, somewhat
sensitive to pressure on the slab. However, they do indicate the
magnitudes of the effects involved.

As will be discussed below, certain ceramics have the proper
high temperature capabilities to be used as closure materials. In
general, these have higher dielectric constants than those of the test
dielectric sheets. The use of foaming techniques can reduce their
density and permitivity. However, bonding and sealing techniques for
high temperature operation of such foamed ceramics are not available.
Therefore, other configurations were considered and are described in
the following sections.

SLOT CLOSURE STUDY

In this section of the report a study is presented on the develop-
ment of slot closures ultimately intended for a flat plate antenna capable
of operation at 2500°F. Vacuum tight slot windows were prepared by
hot press diffusion bonding of mullite to molybdenum. Other techniques
considered for slot closure preparation included mechanical seals,
glazed waveguide, ceramic waveguide and special composites.

High temperature waveguides were made by electron beam welding
of molybdenum sheet to form the rectangular section and then electron
beam welding the slot closure in one end. The external surfaces were
molybdenum disilicided by the diffusion process to provide oxidation
resistance.

11

MATERIALS SELECTION

1. Ceramics

Ceramic dielectrics capable of long term operation at 2500°F include alumina, beryllia, magnesia, spinel, mullite, zircon, fused silica, and several composite compositions. Table 1 lists several of these high temperature dielectrics along with their approximate melting or softening temperatures and room temperature values of their relative permitivities. The melting points of these ceramics are only approximate since these materials tend to soften gradually rather than to undergo a definite change of phase. The dielectric constants are functions of material density and impurities and, as a result, values quoted vary from reference to reference. In addition to variations due to these causes, the relative permitivities also increase with increasing temperature.

Dielectric	Melting or softening point °F	ϵ/ϵ_o 68°F
Alumina	3700	9.7
Beryllia	4650	6.1
Mullite	3290	6.8
Silica	3037	3.7
Zircon	4100	8.4

Table 1. Properties of high temperature dielectrics.

Materials deemed most applicable to this program were zircon and mullite, because of close thermal expansion matching with molybdenum, and alumina because of exceptional dielectric properties at elevated temperatures. Major emphasis was placed on these three materials. Cursory analytical studies only were made with other materials. Several curves of thermal expansion properties of ceramics and high temperature metals are shown in Figure 2a through 2i.

12
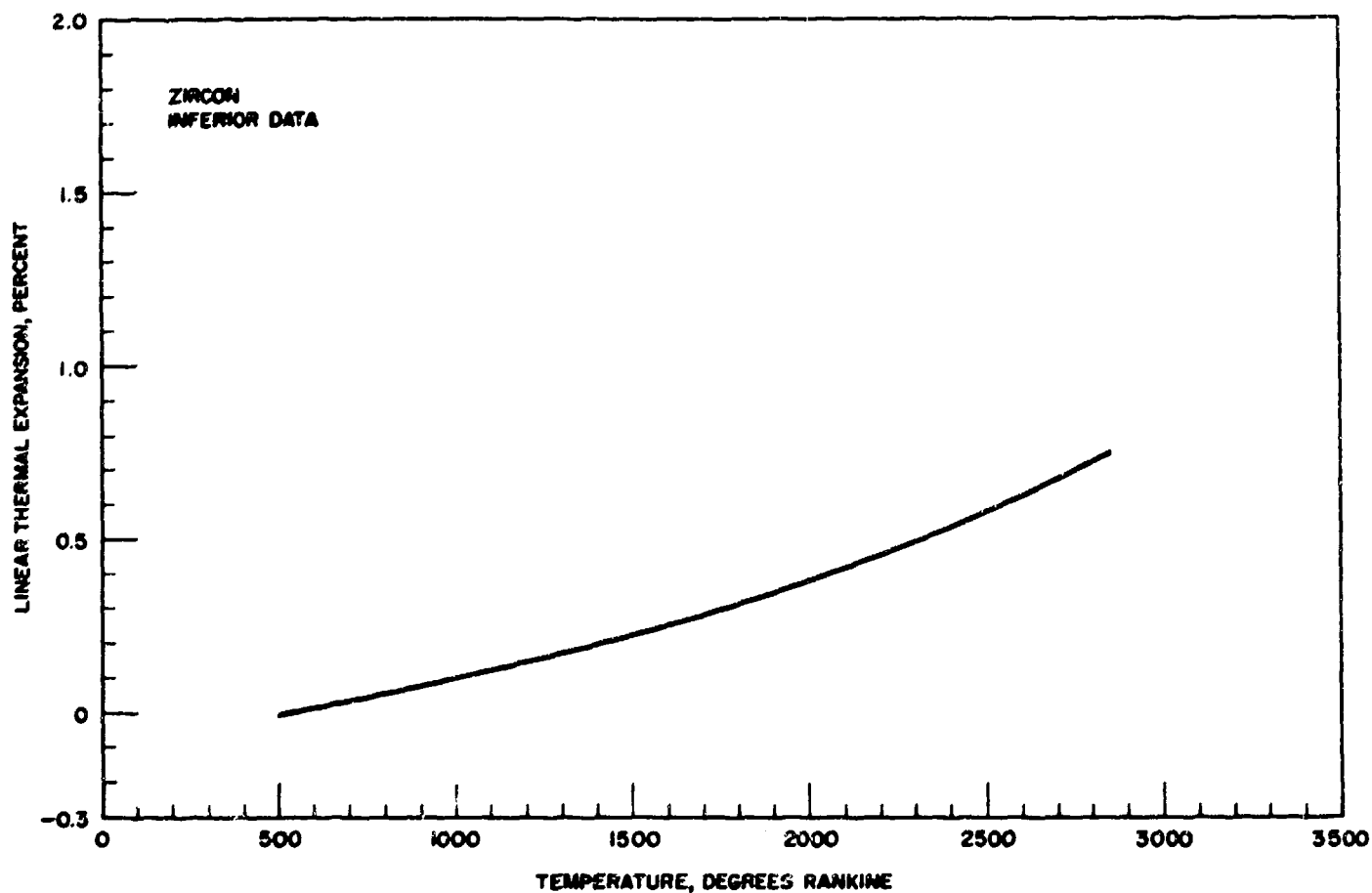
Figure 2a. Thermal expansion properties of high temperature materials.
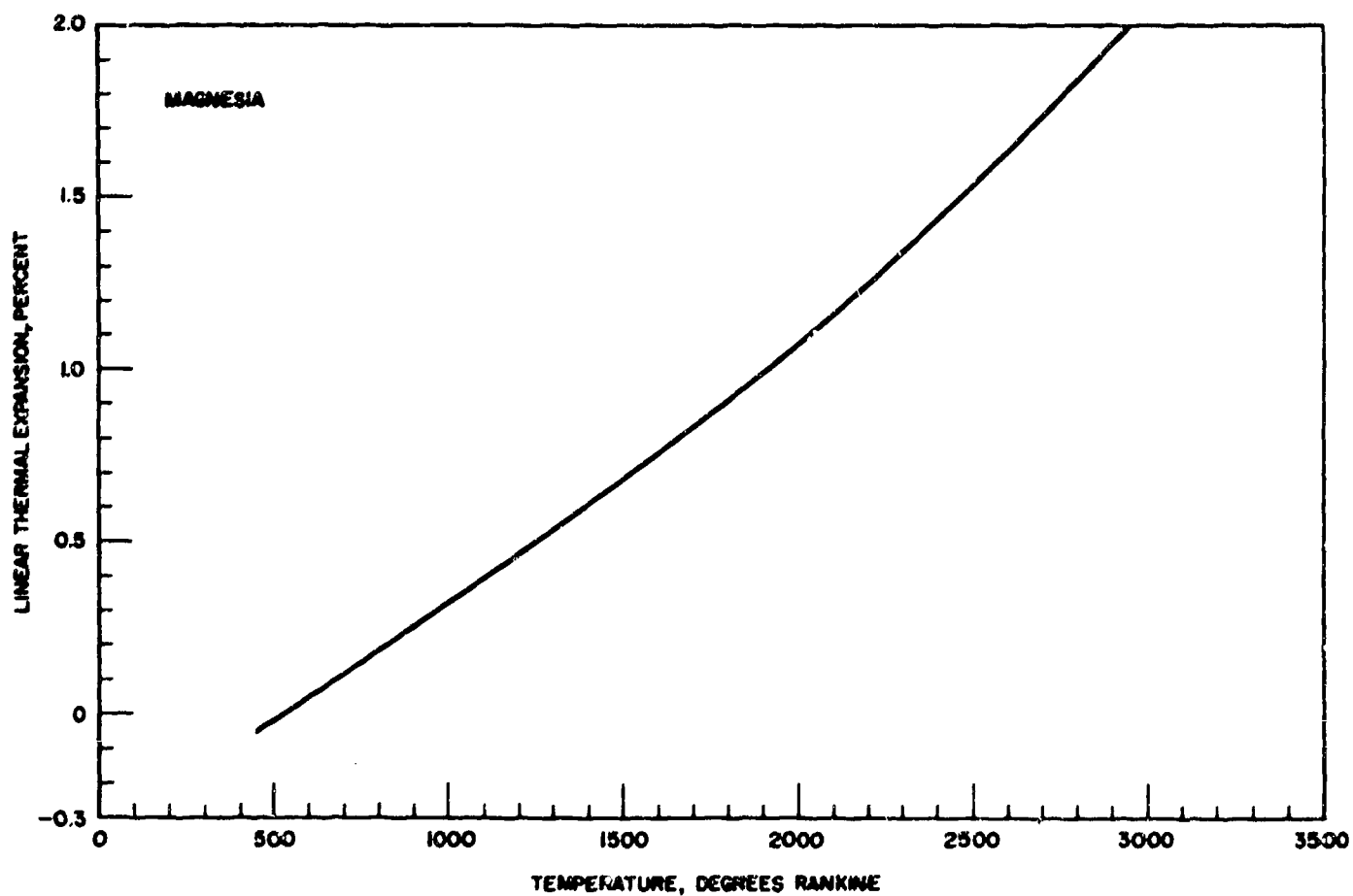
Figure 2b. Thermal expansion properties of high temperature materials.

13
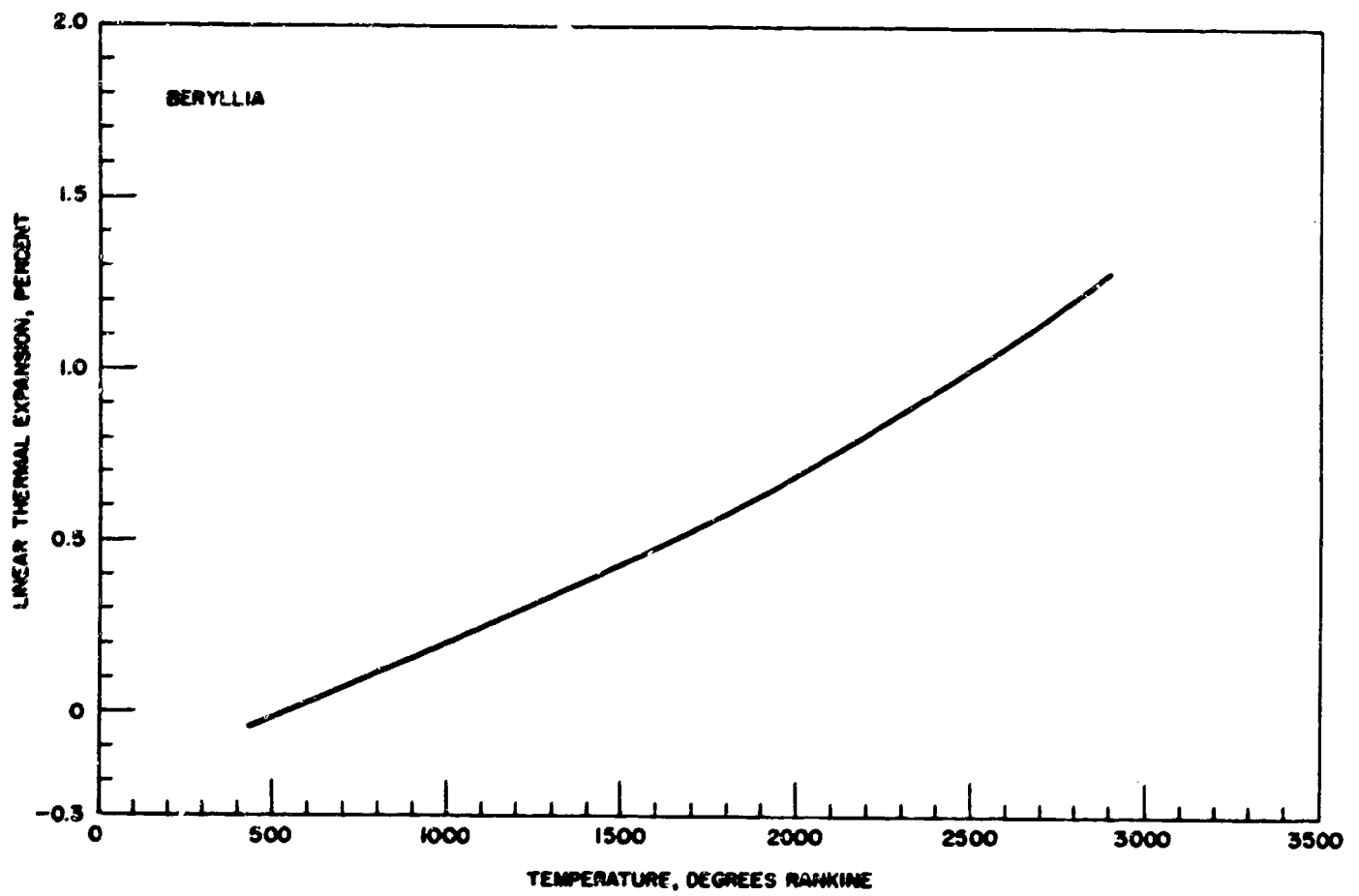
Figure 2c. Thermal expansion properties of high temperature materials.
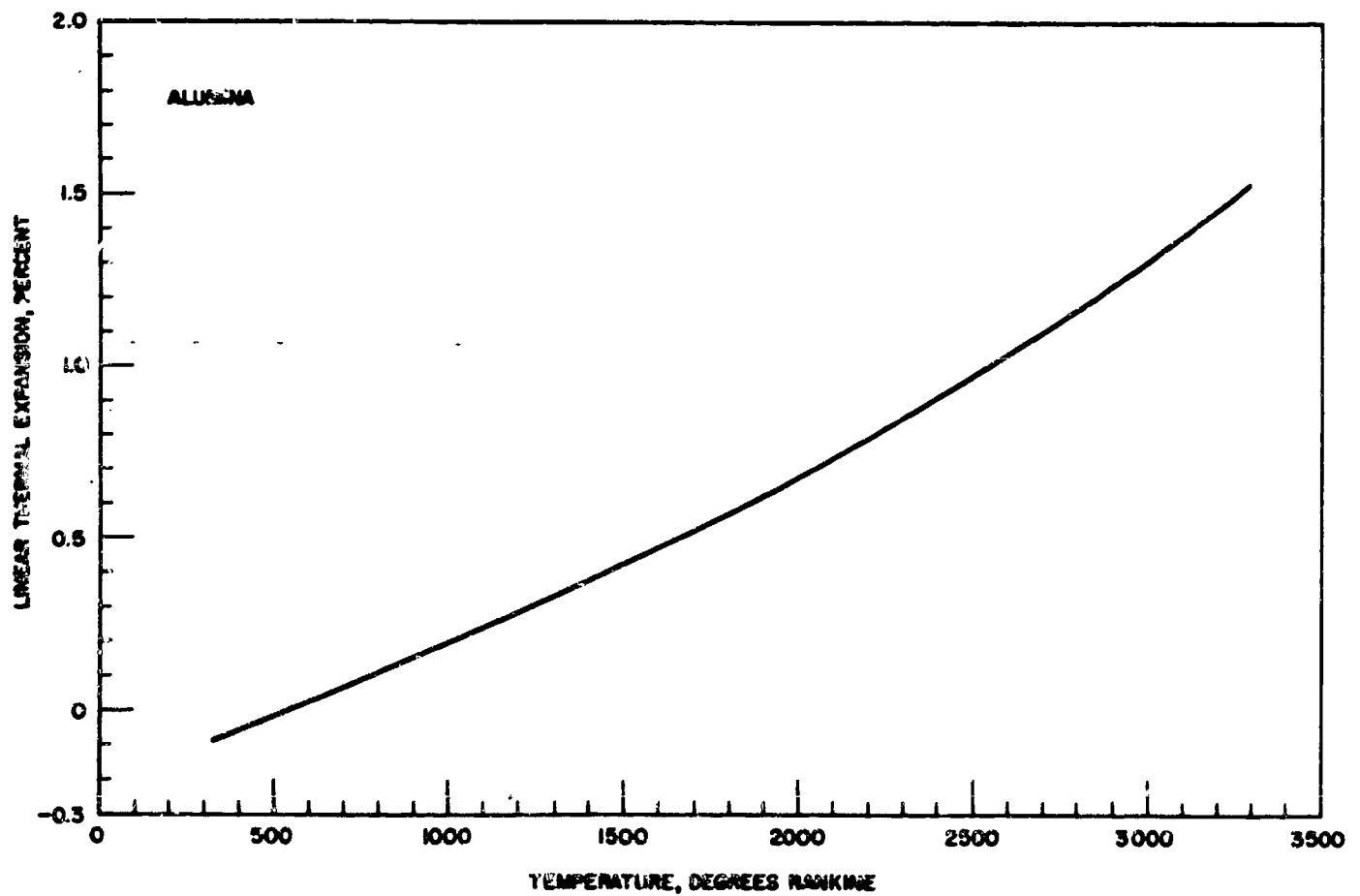
Figure 2d. Thermal expansion properties of high temperature materials.

14
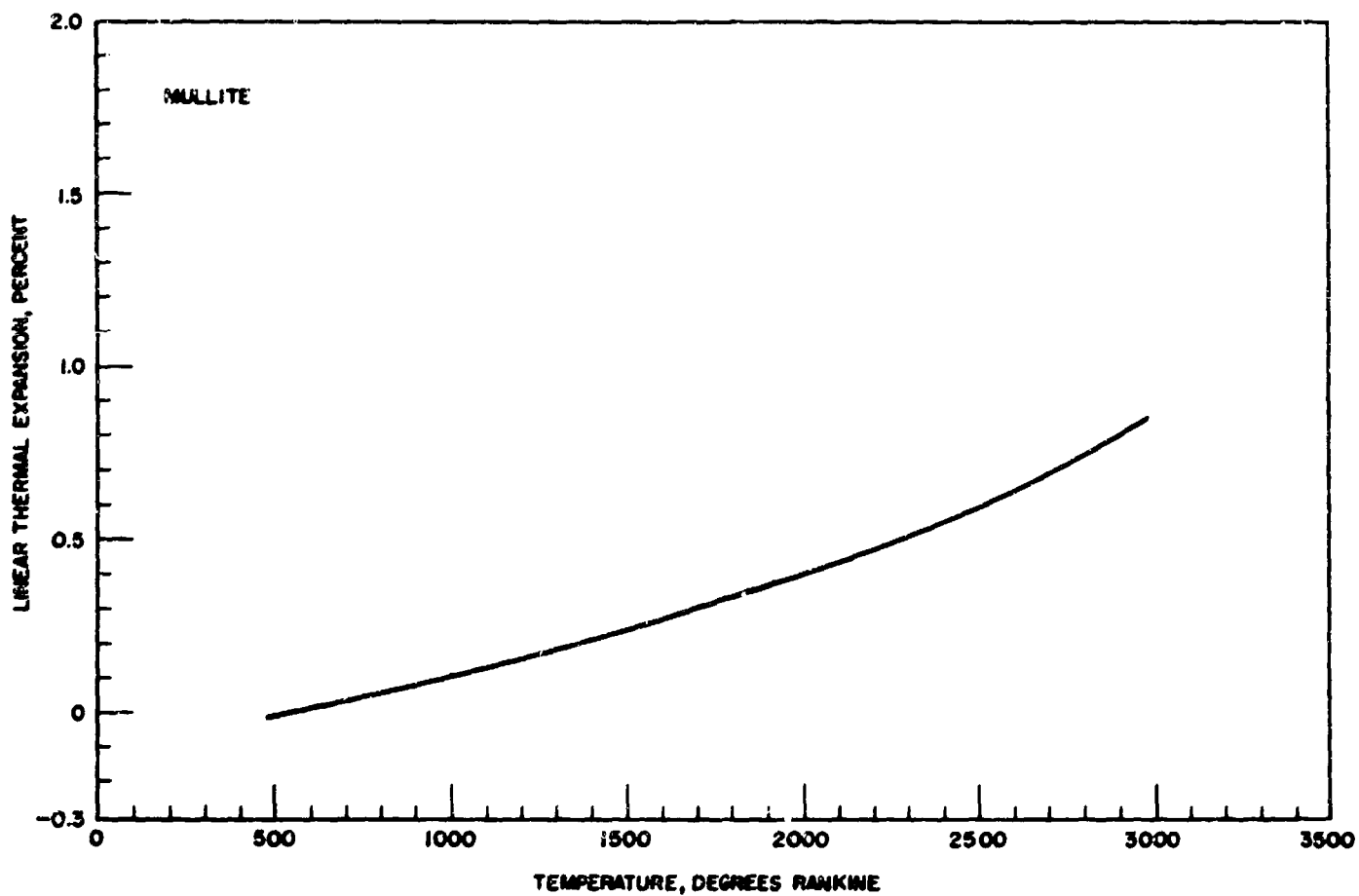
Figure 2e. Thermal expansion properties of high temperature materials.
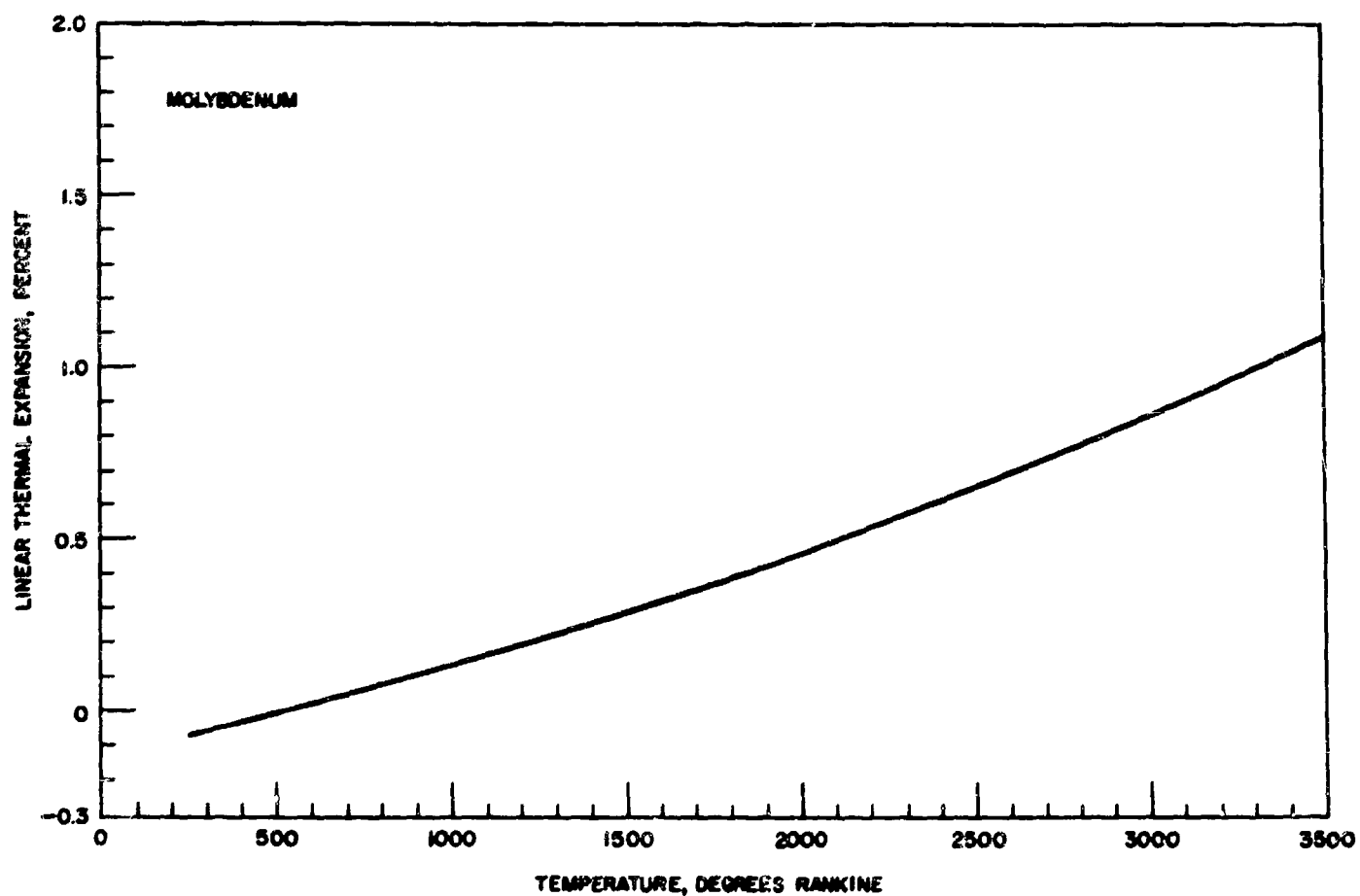
Figure 2f. Thermal expansion properties of high temperature materials.

15
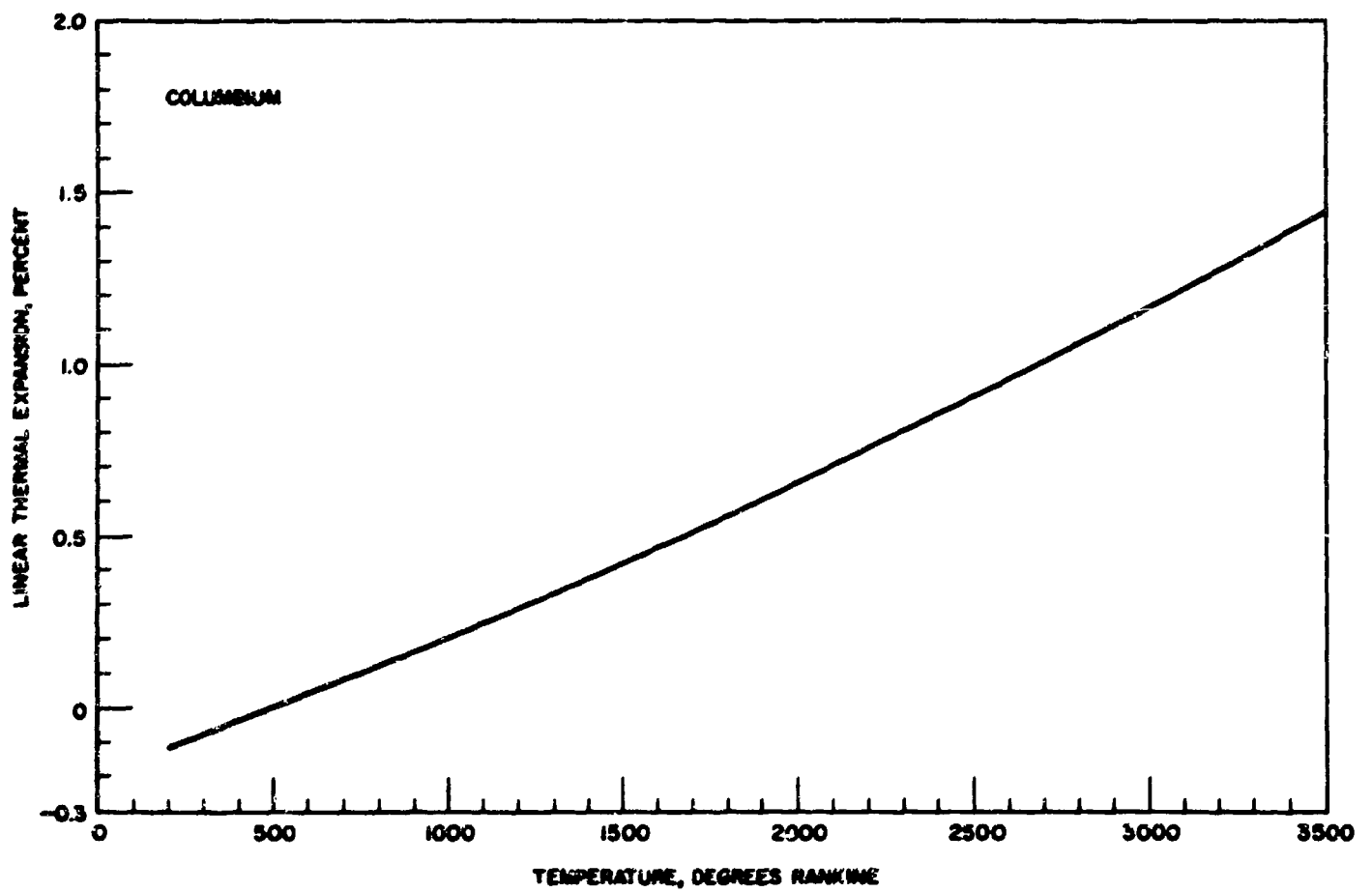
Figure 2g. Thermal expansion properties of high temperature materials.
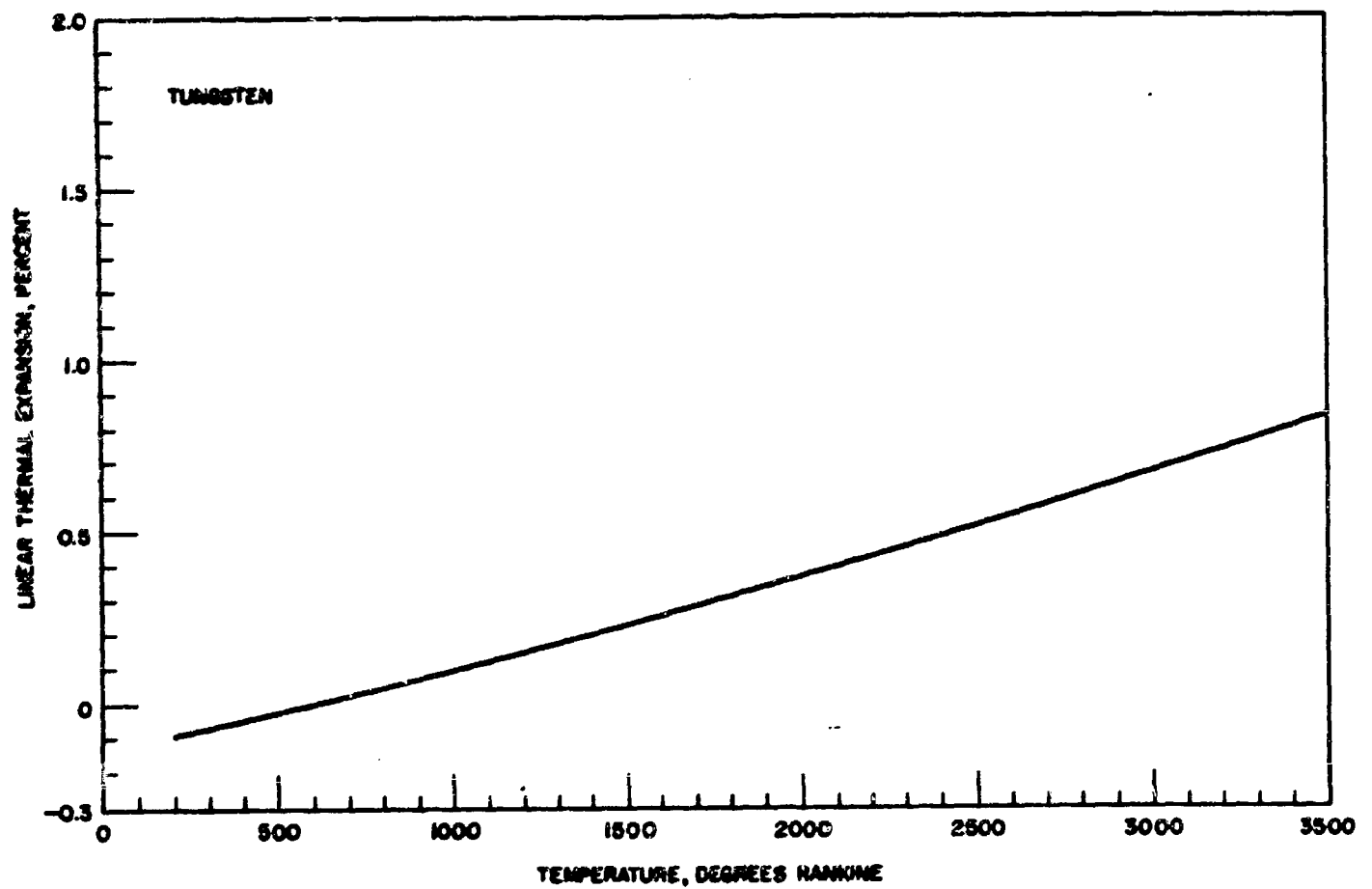
Figure 2h. Thermal expansion properties of high temperature materials.

16
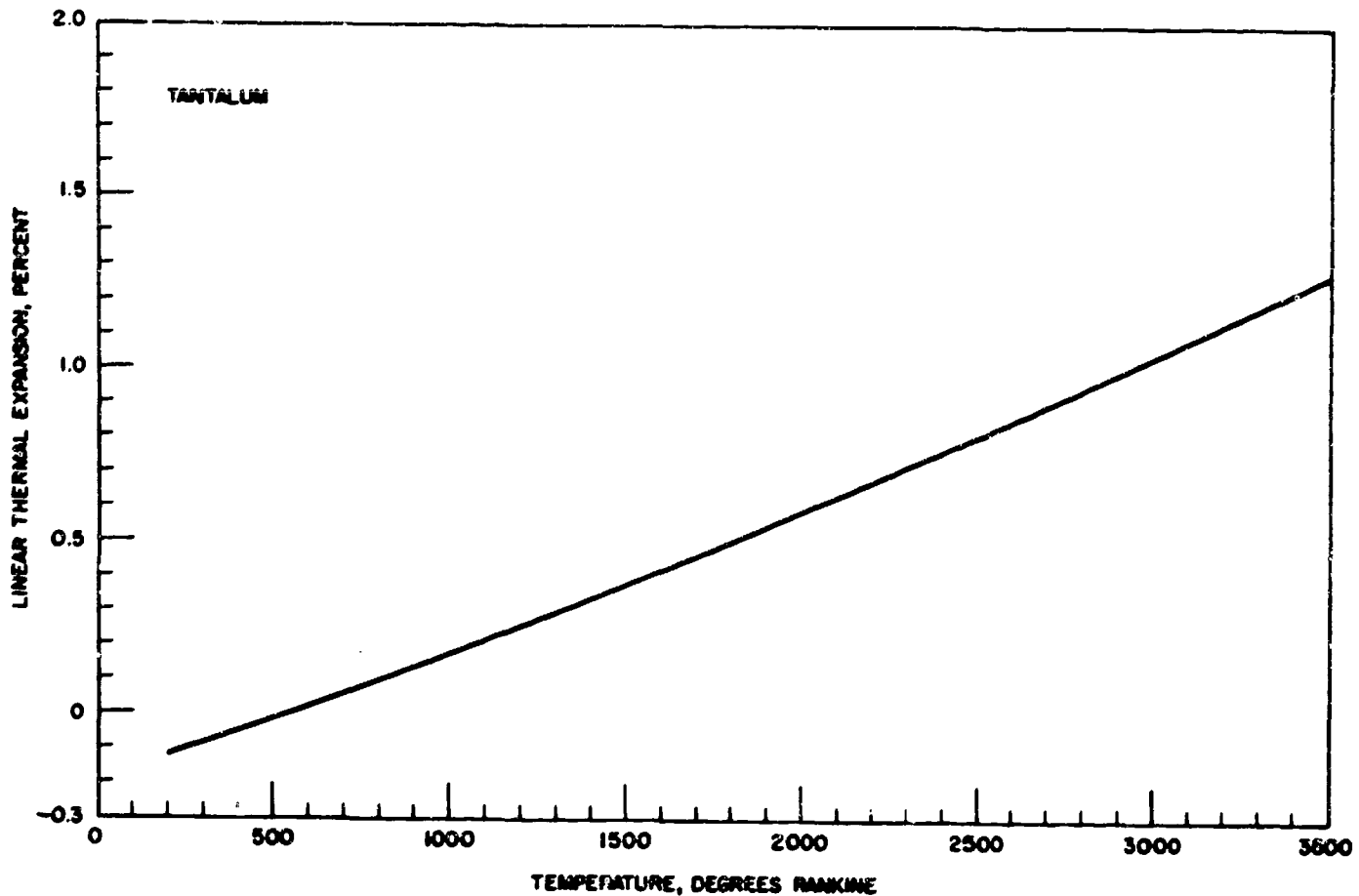
Figure 2i. Thermal expansion properties of high temperature materials.

2. Metals

The primary considerations in selection of the metallic material for the waveguides were: (1) high temperature capability, (2) coefficient of expansion matching that of the dielectric material, (3) density, (4) the ability to apply an oxidation resistant coating, (5) fabricability, (6) availability, and (7) cost. Electrical conductivity is important also, but the other requirements restrict the choice of materials to those that do not have exceptional electrical conductivity. The only materials that meet these requirements are refractory metals and alloys and certain precious metals. The former depend upon oxidation resistant coatings for high temperature service while the latter are oxidation resistant.

17

Table 2 lists the higher temperature metallic elements by approximate melting temperatures in decreasing order.[2,3] Copper and aluminum are included at the bottom of the list for comparison. Also given are density, electrical resistivity at both room temperature and 2500°F, and finally, the approximate cost per pound of the material in bulk (ingot) form. Since many of these metals are difficult to fabricate, the cost of sheet and mill stock can be considerably higher than bulk material. Of all the high temperature metals listed, molybdenum probably has the most developed technology at this time.

Metal	Melting point °F	Density lb/cu in.	Electrical resistivity ohm-cm at		Approximate Cost $/lb
			68°F	2500°F	
Tungsten	6170	0.697	5.5	45	4
Rhenium	5755	0.756	16	90	600
Osmium	5432	0.815	60	--	1500
Tantalum	5425	0.600	14	65	50
Molybdenum	4730	0.369	5.7	35	4
Columbium	4474	0.310	15	70	40
Iridium	4449	0.813	6	--	1500
Ruthenium	4082	0.441	6	58	1000
Hafnium	4032	0.473	32	160	40
Rhodium	3571	0.447	5	--	2000
--					
Copper	1981	0.323	1.7	--	0.3
Aluminum	1220	0.098	2.8	--	0.3

Table 2. Properties of high temperature metals.

The electrical losses in waveguide are proportional to the surface resistivity of the guide walls. This surface resistivity is given by the following equation

$$R_s = \sqrt{\pi f \mu \rho}$$

where R_s is the surface resistivity in ohms per square, f is the frequency in cycles per second and μ and ρ are, respectively the permeability and volume resistivity of the material expressed in compatible units. It is apparent from the equation that losses do not increase rapidly as the material volume resistivity increases. For example, based on the values shown in Table 2, the losses of a molybdenum waveguide at 2500°F are only about 3.5 times as great as those of aluminum guide at room temperature. At 8.2 Gc this gives an attenuation of about 0.2 db per foot which is not intolerable for moderate size antennas in such an extreme temperature environment.

Disregarding precious metals from cost and availability stand-points, molybdenum or columbium were the preferred metals of the refactories. There are some tradeoffs in the selection of one of these metals over the other. Molybdenum was chosen on the basis of a co-efficient of expansion closely matching that of the ceramics intended for the slot closures and because the oxidation coating technology is further advanced for molybdenum. Columbium has the advantages of better fabricability based on its ductility and also it retains its ductility after heating to 2500°F.

HOT PRESSING STUDIES

A laboratory hot press (Figure 3) was utilized for development studies in diffusion bonding between molybdenum and ceramic powders. Pressing studies were first made using ceramic powders only to establish pressures, times, and temperatures for preparation of strong nonporous specimens with a minimum of carbon contamination. Schedules for powder pressing are shown in Table 3. Hot pressed ceramics are shown in Figure 4.

19
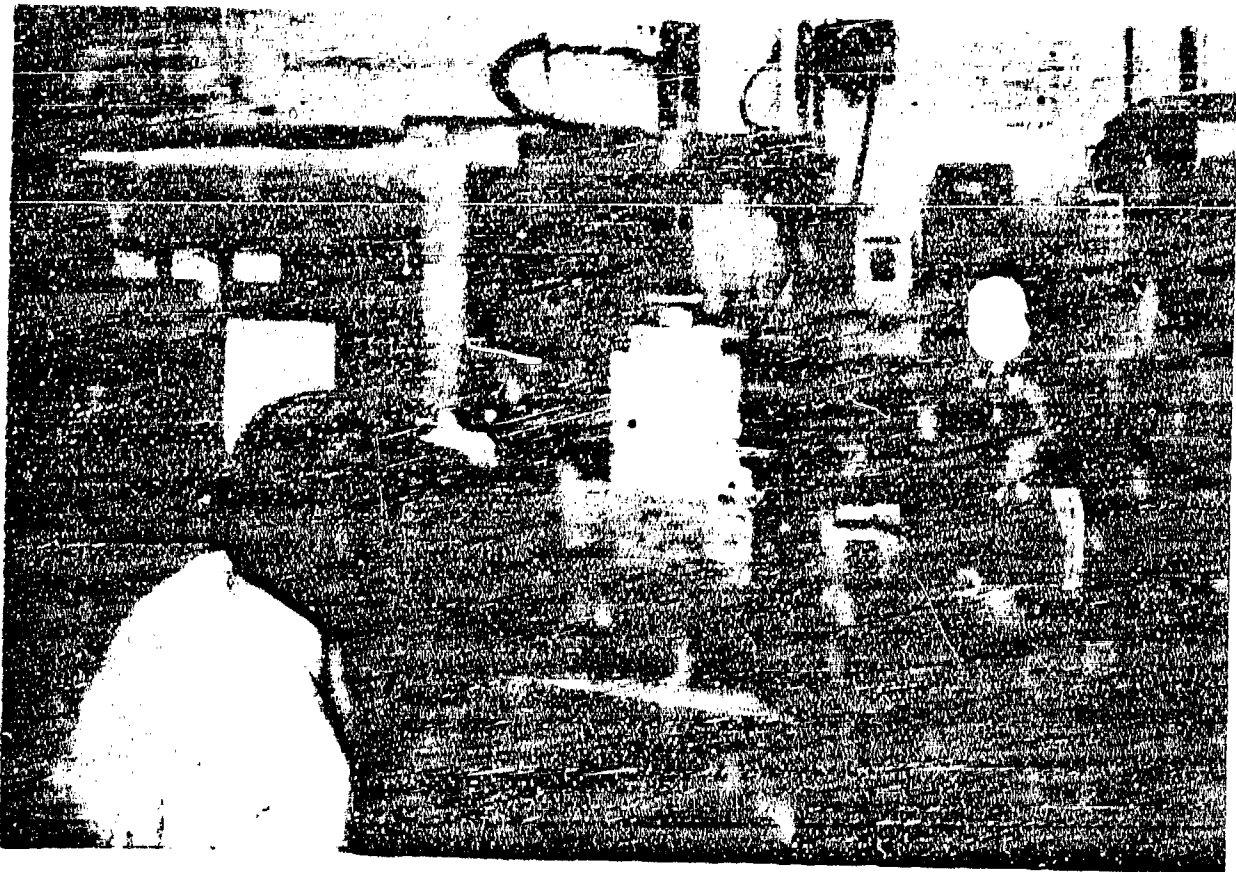
Figure 3. Laboratory hot press facility.
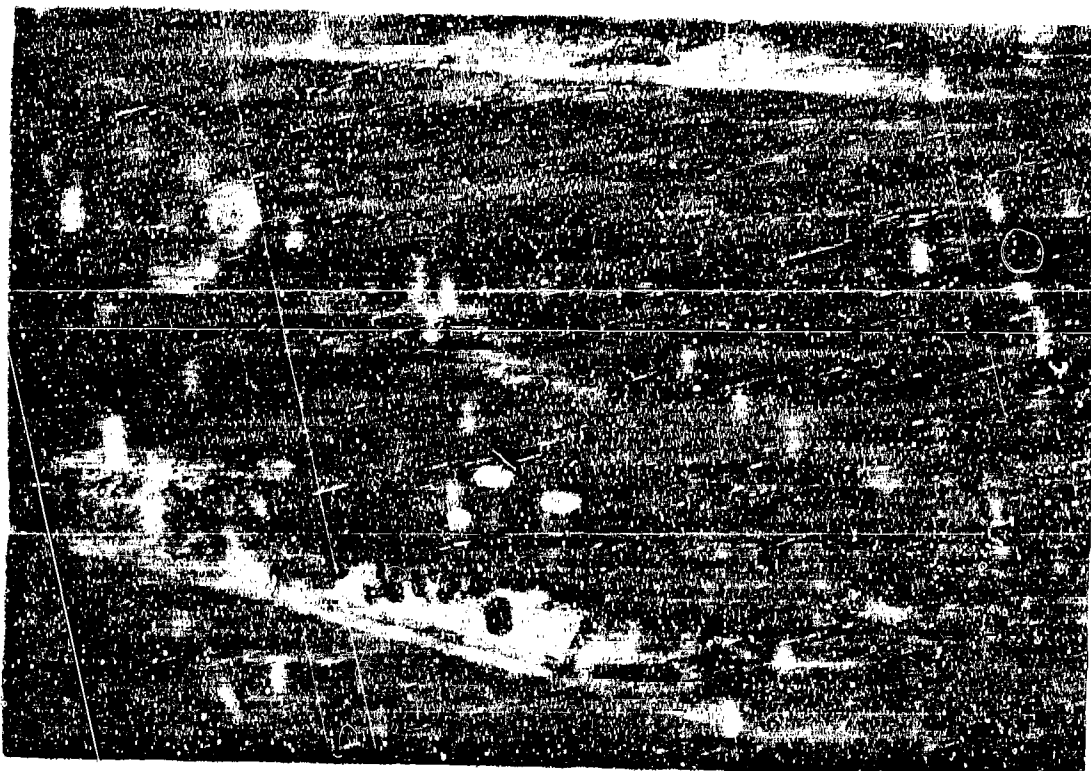
Figure 4. Hot pressed ceramic components and graphite dies.

	Mullite	Zircon	Zircon
Temperature, °C	1600	1600	1600
Pressure, (psi)	4500	4000	3300
Time, Min	10	10	10

Table 3. Hot pressing parameters for preparation of ceramic dielectric specimens.

Diffusion bonds were then attained between zircon and molybdenum and between mullite and molybdenum. Alumina was bonded to molybdenum using a thin platinum interlayer. After attainment of successful bonding to the metal, alumina was found to be poorly matched in thermal expansion with molybdenum. Specimens generally cracked upon removal from the press, or upon cool-down to room temperature. Fragments, however, were well bonded to the metal.

The use of a thin (0.002 inch) layer of platinum was found highly desirable for obtaining more reliable bonds between molybdenum and mullite. An excellent diffusion bond between mullite and molybdenum may be seen in Figure 5. One zircon window bonded directly to molybdenum with platinum at the interface, and two mullite windows were checked for helium leak tightness before and after heating. All windows were helium leak tight before heating. After heating the zircon window to 2690°F, leakage was excessive. The two mullite windows were heated to 2720° and to 2910°F before retesting. The former showed a slight leakage; the latter was helium leak tight. Difficul⁺ was experienced in pressure bonding of zircon to molybdenum due to the reactivity of zircon with carbon vapors from the graphite die. This resulted in bonding between zircon and the graphite plungers with subsequent deterioration of the die. Major effort was therefore directed towards mullite windows where this problem was not encountered. Also, the dielectric properties of mullite are expected to be better than those of zircon at 2500°F. Hot pressed mullite windows may be seen in Figure 6.
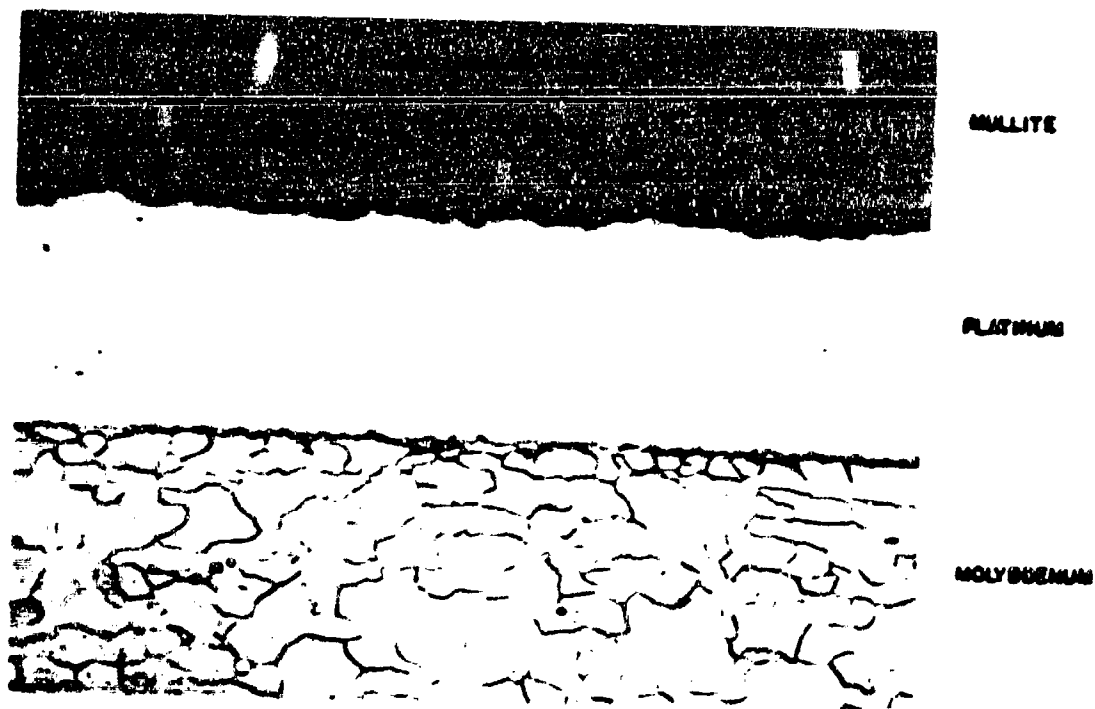
Figure 5. Mullite-Platinum-Molybdenum interface
of hot pressed slot enclosure. Magnification
200 times.

Figure 6. Hot pressed mullite windows in
Molybdenum end plates.

Transmission measurements were made on one finished mullite
window before and after application of the molybdenum disilicide pro-
tective coating. This was done to determine if there was an interaction
between the ceramic window and the metal protective coating process.
Discoloration of the ceramic was noted, the edges of the molybdenum
were extremely brittle and appeared to exfoliate. This was due to dif-
fusion of the disiliciding vapors between the lamellar structure of the
molybdenum. By deburring and rounding off edges, however, this
problem was alleviated.

MECHANICAL SEAL

Ceramic discs of alumina, mullite, and zircon were procured for
preparation of mechanically sealed end plates. The discs were 0.375
inch diameter by 0.050 inch thick. Molybdenum waveguide end plates
were prepared from 0.050 inch stock, and 0.375 inch holes were
machined in their centers.

The end plates were heated to 800°F, providing a diametrical
difference of about 0.001 inch. The cold ceramic discs were pressed
into the hot end plates, and the m' ₁ shrank to the dimension of the
ceramic. These end plates are shown in Figure 7. These seals were
prepared for measurements of transmission properties at 2500°F, and
were not intended to be helium leak tight. High temperature measure-
ments were not made, since the success with hot pressed specimens
eliminated the necessity of continuing the effort with mechanical sealing
techniques.

GLAZED WAVEGUIDE

Several high temperature glass compositions were previously
developed by the Ceramics Group for fiber usage. These compositions
appeared promising for dielectrics. Expansion coefficients were calcu-
lated, and three glasses were selected for adherence studies to molyb-
denum. Glass compositions, fusion points, and calculated thermal
expansion coefficients are shown in Table 4.
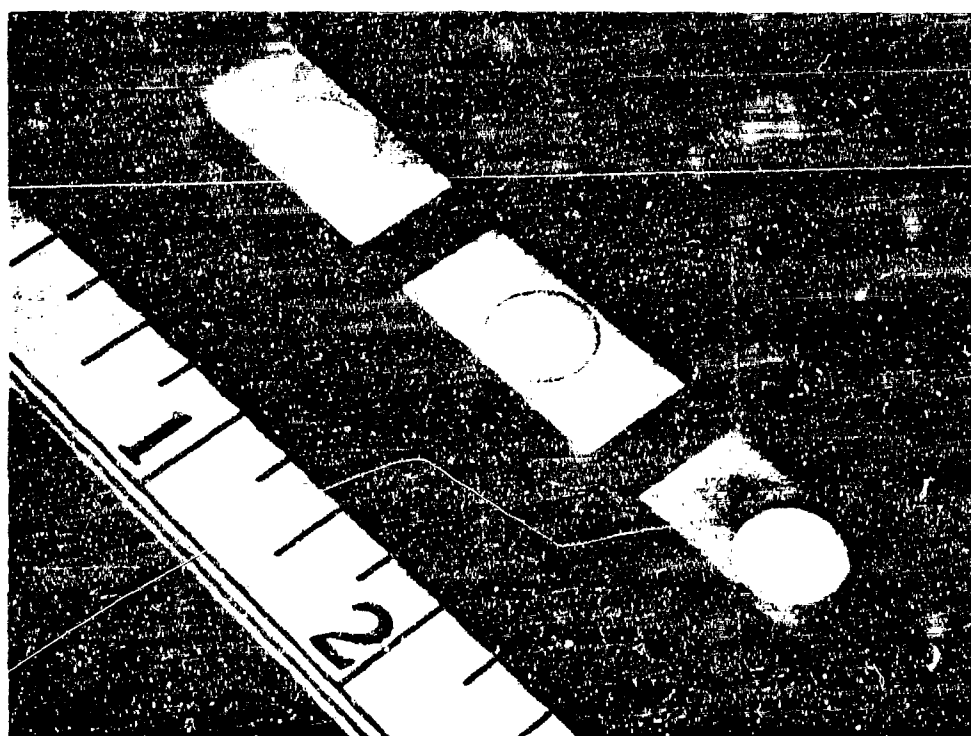
Figure 7. Mullite, Zircon, and Alumina
windows shrink fitted into
Molybdenum end plates.

Glass No.	Constituent	Amount (%)	Fusion Temperature (°C)	Thermal Expansion (in./in./°C)
R45	SiO_2	36.0	1475	6.40×10^{-6}
	Al_2O_3	48.0		
	MgO	16.0		
R74	SiO_2	50.0	1450	5.18×10^{-6}
	Al_2O_3	22.5		
	MgO	7.5		
	ZrO_2	20.0		
R99	SiO_2	50.0	1580	4.99×10^{-6}
	Al_2O_3	27.0		
	MgO	3.0		
	ZrO_2	20.0		

Table 4. Characteristics of high temperature glasses.

Rods were prepared from the glass compositions and fritted using an induction heated apparatus. The frits were ground into fine powder or prepared as slip and applied to molybdenum test strips. Heating was accomplished using a laboratory resistance heated vacuum furnace. Because of the vacuum, and the high temperatures involved, it was generally difficult to achieve glaze maturity without boil off or bubble formation. Thin and thick powder coatings were used as well as sprayed aqueous coatings. In general, the fit was good, and subsequent heating in a helium atmosphere yielded promising coatings.

Several of the better coatings were heated in air to 2500°F for one minute. It was difficult to estimate the degree of metal protection afforded by the glaze, but it was found that glaze number R-74 was soft at 2500°F, and should be discarded from consideration. Both of the compositions (R-45 and R-99) were hard at this temperature. A section of glazed molybdenum before and after exposing to 2500°F in air is shown in Figure 8.
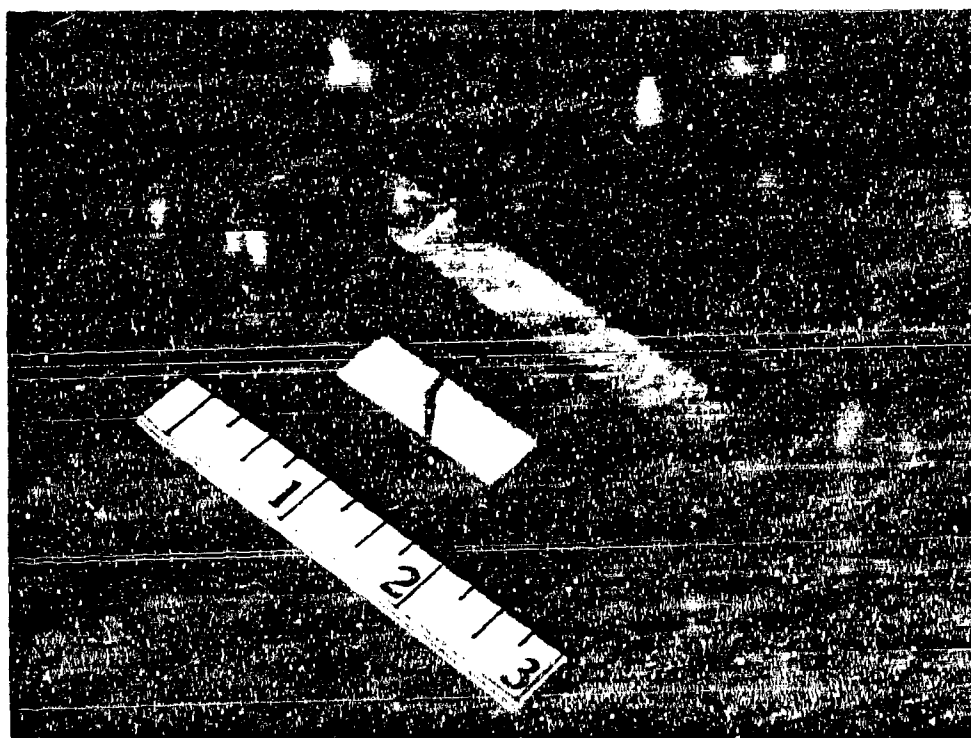
Figure 8. Glazed Molybdenum sections before and after exposure to 2500°F in air. Glaze was soft at 2500°F, as shown by scratch.

25

Initial attempts were made to prepare ceramic waveguide using wax mandrels. Standard alumina slip was found to be unsuitable due to shrinkage cracking.

A special alumina spraying slip was prepared with an organic binder and an alcohol vehicle. This material was sprayed onto a heavily waxed mandrel. As the particles traveled from the spray gun to the mandrel, the alcohol evaporated so that the particles stuck tightly and built up a thick layer with no drying shrinkage. The formed waveguide section was easily removed from the mandrel by gently warming and melting the wax. The piece was fired and is shown in Figure 9. The internal geometry was maintained precisely. The process is very promising for fabricating ceramic waveguide with the required internal tolerances. Flanges may be fabricated as an integral part of a waveguide section.
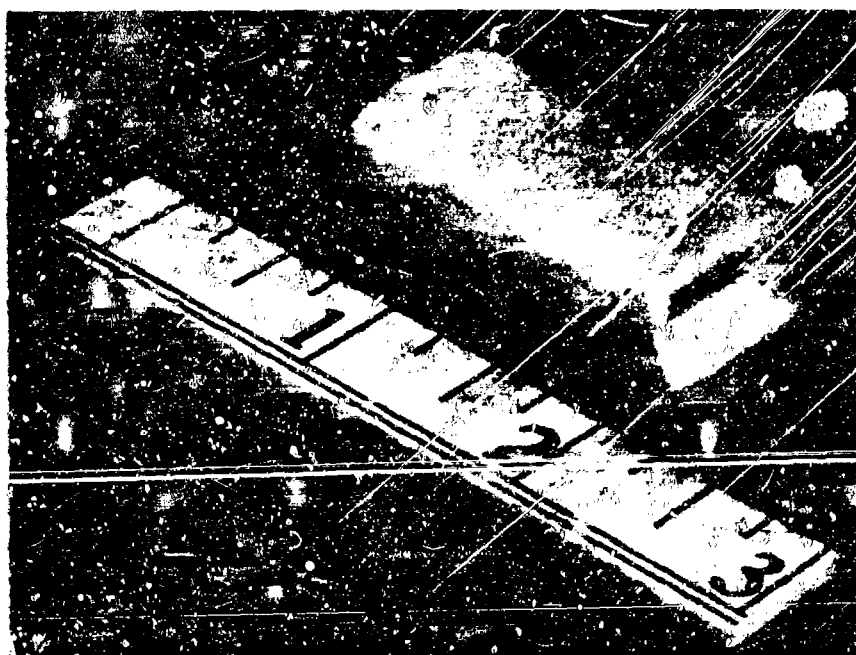
Figure 9. Alumina waveguide section.

A more or less conventional method was also considered for slip casting mullite waveguide with an integral flange. A mold design was established for casting precision sections to close tolerances. The special features of this mold included presoaking the mold and utilizing a collapsible core. No laboratory effort was expended on this.

Ceramic cements, including Sauereisen and aluminum phosphate, were found to have insufficient adherence to molybdenum at $2500^{\circ}F$ to warrant further consideration. High temperature glasses have excellent adherence, but offer no advantages over diffusion bonding. Mullite and zircon specimens that were successfully bonded to molybdenum with a refractory glass are shown in Figure 10.

Boeing has reported use of Sauereisen No. 77 for bonding ceramics to molybdenum. The process was reported to be pressure tight at room temperature, and reported to perform satisfactorily at high temperature.

Figure 10.   Mullite and Zircon windows
attached to Molybdenum
strip with glass adhesive.

FABRICATION OF METALLIC WAVEGUIDE SECTIONS

1.   Gas Pressure Bonding

This process in which metal to metal or metal to ceramic bonds are obtained by solid state diffusion was considered in the initial stages of this study. This process was attractive because it offered a means of both bonding the ceramic slot closure and providing external oxida-

tion resistance by ceramic coating the waveguide in one operation. This process was rejected because of schedule problems.

2. Forming by Vapor Deposition

In this process, metallic shapes are made to close tolerances by deposition of metal on a mandrel of the desired configuration. A molybdenum compound in the vapor state is passed over the heated mandrel and upon impinging on the mandrel, the compound decomposes depositing dense molybdenum on the mandrel. This process has a great deal of flexibility insofar as complex configurations are concerned. Efforts by an outside vendor to make waveguide sections by this process were unsuccessful because the waveguides stuck to the mandrels which caused cracking of the waveguides as the steel mandrel shrank at a greater rate than the molybdenum upon cooling. This problem probably could have been solved if the limited schedule had permitted experimentation with other mandrel materials or parting agents.

3. Electron Beam Welded Structure

Molybdenum waveguides were made from 0.040 inch sheet by electron beam welding. Steps 0.015 inch deep were machined in the edges of the sheets so that they were self-jigging to form the rectangular box configuration of the waveguide. Electron beam welds were made on the four edges. The end plates with the hot pressed ceramic window were machined with a step around the perimeter so that they were self-locating in the end of the waveguides. The end plates were then electron beam welded to the waveguide. A characteristic of electron beam welds is a high depth to width ratio of the weld with consequent low heat input and minimum thermal distortion. There was a minor amount of distortion from welding. This distortion was removed by creep forming the waveguides by placing steel plates on them in a hydrogen atmosphere furnace at 2000°F for 1 hour. After this treatment, the dimensions conformed to those specified in Figure 11. Figure 12 shows one of the waveguides after welding.

0.350"±0.002"

0.0625"±0.001"SLOT LOCATION WITHIN 0.003" OF ₵
AS MEASURED FROM INSIDE DIMENSIONS
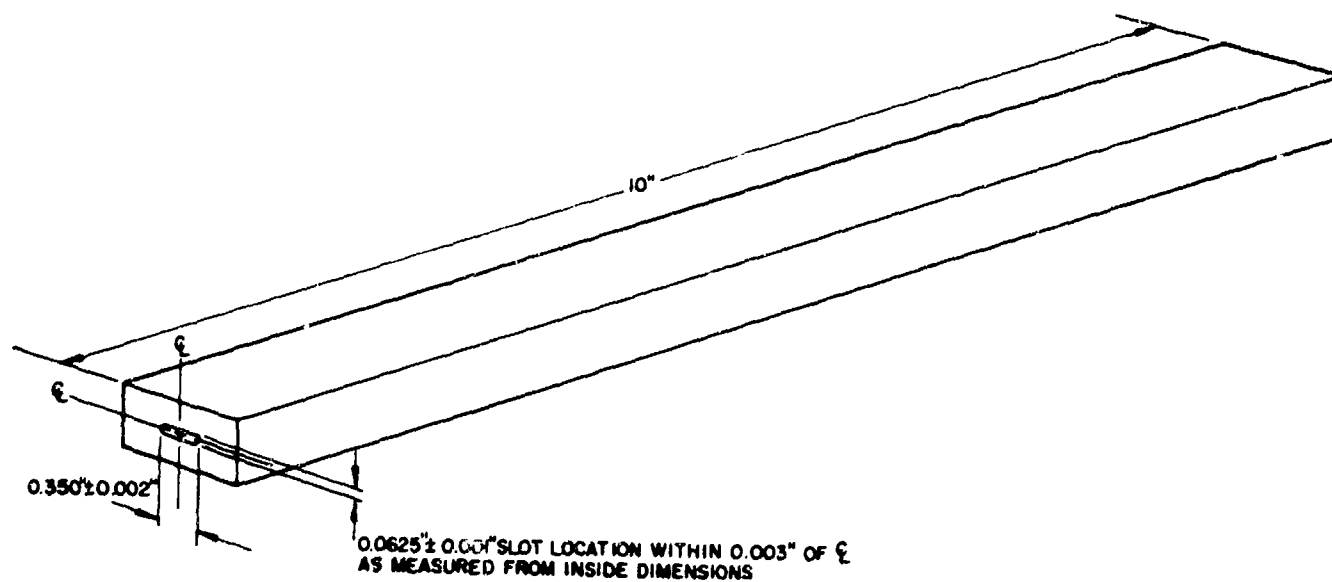
GENERAL NOTES:
1. WAVEGUIDE I.D , 0.400"x 0.900"±0.003"
2. WAVEGUIDE WALL THICKNESS , 0.040"±0.003"
3. MAXIMUM AXIAL CAMBER , ±0.003" OVER ENTIRE LENGTH
4. 1/32"MAXIMUM RADIUS ON ALL INSIDE CORNERS
5. INSIDE SURFACE FINISH 32 rms

Figure 11. High temperature waveguide test section.
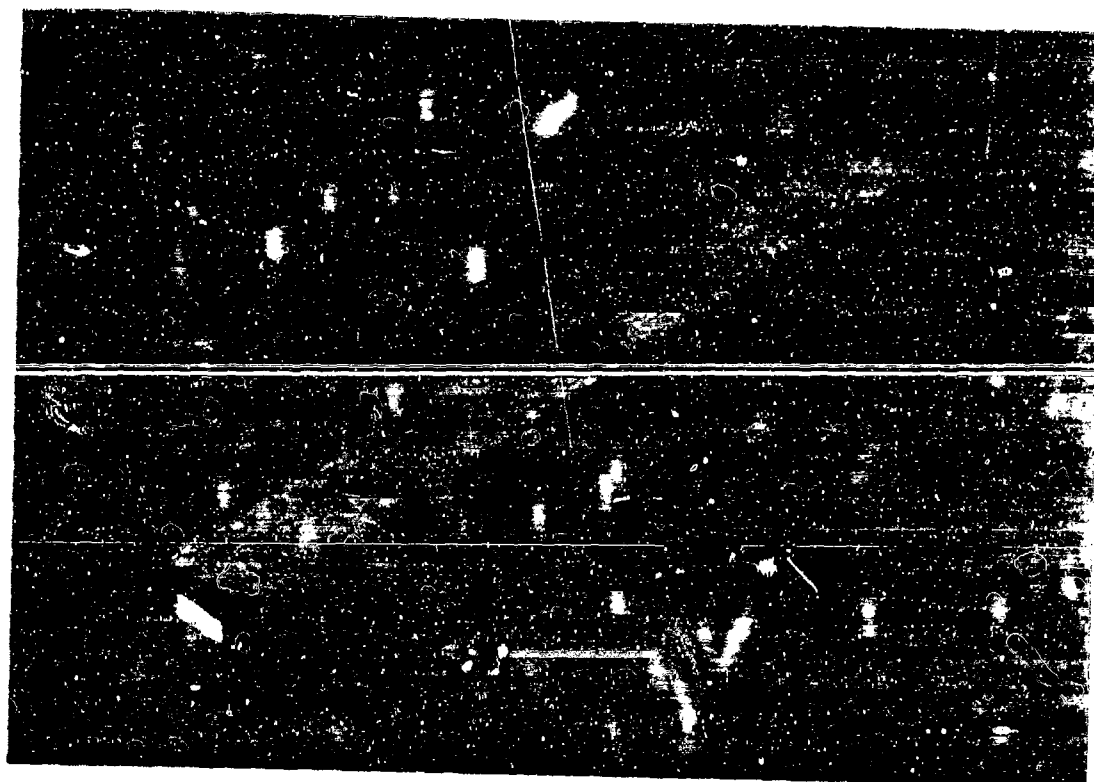

Figure 12. Welded waveguide.

29

4. Oxidation Protection

A molybdenum disilicide diffusion coating was applied to the external surfaces of one of the waveguides. Some discoloration of the mullite window occurred during the disiliciding process. It was no longer optically translucent. This may be due to a shallow surface reaction and possibly it can be removed by selective abrasive cleaning. In the hot pressing operation, the platinum apparently was extruded around the edge of the window. There appeared to be a reaction between this platinum and silicon fluoride used in the coating process. The interior of the waveguide was filled with inert material to prevent the coating of the inside surfaces. The purpose of leaving the interior bare is to achieve the best electrical conductivity. Molybdenum is reported to have a resistivity of 35 micro-ohm-cm at 2500°F and molybdenum disilicide has reported resistivity values ranging from 80 to 300 micro-ohm-cm at 2500°F. In elevated temperature testing the waveguides would be pressurized with dry inert gas to prevent oxidation of the internal surfaces.

Flanges would be silver brazed onto the waveguides and copper cooling coils would be brazed to the flanges to keep the flange end cool during elevated temperature testing where the slotted end of the waveguide is inserted in a furnace as shown in Figure 13. Tests have indicated that molybdenum — disilicide coated metal is readily silver brazed.

EVALUATION

Thermal Shock Tests

One zircon and two mullite windows, diffusion bonded to molybdenum end plates, were helium leak checked before and after thermal shock testing. All specimens were helium leak tight before thermal exposure. The zircon window was uniformly heated to 2690°F within five minutes and allowed to cool to room temperature. A bubble or void was noticed at the metal ceramic interface, and the specimen leaked badly when tested. One mullite window was heated to 2720°F; the other was heated to 2910°F, each within five minutes. After cooling to room temperature, it was noted that the specimen heated to 2720°F had a

30

small chip at the edge of the ceramic. Slight helium leakage was detected. The specimen fired to 2910°F appeared sound, and subsequent testing showed it to be helium leak tight.

Transmission Measurements at Room Temperature

Dielectric transmission measurements were made on a bonded mullite window before and after application of the molybdenum disilicide coating with which the molybdenum waveguide is to be protected from oxidation. A four db decrease in transmission was noted, and is attributed to non-uniformities in the disilicide coating around the window, reactions between the ingredients of the disilicide process and the mullite, and the change in electrical resistance of surfaces of the molybdenum after coating.

Table 5 lists the transmission and VSWR measurements made on two electron beam welded molybdenum waveguides with mullite filled slots prior to disiliciding. These waveguides conformed to the dimensional and flatness requirements specified in Figure 11. Figure 14a and b are values of input VSWR of the waveguide window units when radiating into space.

High Temperature Transmission Tests

A Globar heated test facility has been designed for waveguide transmission evaluation at temperature up to 2500°F. The cross section of the facility is shown in Figure 13. However, due to lack of time high temperature tests were not performed.
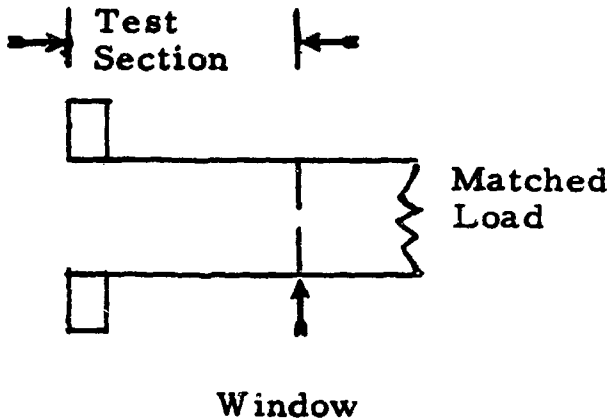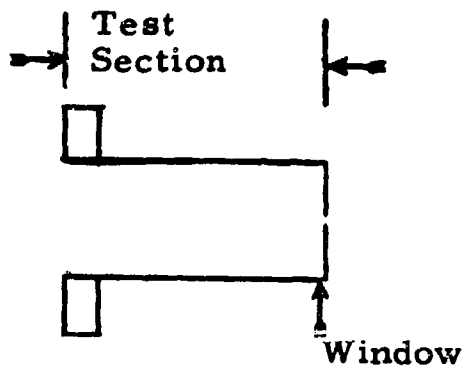
	Sample 1	Sample 2
Case (1)		
Feeding a waveguide with matched load		
Res. Freq. (Min VSWR)	9.120 Gc	9.028 Gc
VSWR	1.235	1.165
Insertion loss db	0.35	0.45
Case (2)		
Radiating into space		
Res. Freq. (Min VSWR)	8.950 Gc	8.876 Gc
VSWR	1.085	1.130

Case 1	Case 2

Table 5. Transmission measurements of molybdenum waveguides with windows prior to disiliciding.

INSULATING FIREBRICK

GLOBAR HEATING ELEMENT

CERAMIC RADOME

CERAMIC SLOT CLOSURE

RECEIVING HORN

MOLYBDENUM WAVEGUIDE

SIDE ELEVATION SECTION

THERMOCOUPLE

Figure 13. 2500°F antenna test facility.

(a) Sample One

(b) Sample Two

Figure 14. Input VSWR of window radiating into space.

BEAM STABILIZATION STUDIES

DETERMINATION OF SCAN REQUIREMENTS

As a reentry vehicle maneuvers it will undergo pitch, roll and yaw motions about axes fixed within the vehicle. As it goes through these motions it is desirable that the beams of a doppler velocity sensor antenna remain fixed relative to a system of reference axes, X_e, Y_e, Z_e. These reference axes are moving with the vehicle but are oriented in such a way that one axis, e.g., the Y_e axis is tangent to a sphere concentric with the earth and lies in the plane determined by the velocity vector and the local vertical. Its sense is along the tangential projection of the velocity vector. A second axis, e.g., the Z_e axis lies along the local vertical and is positive in the downward direction. The third axis, X_e, is defined by requiring the system to be a right handed system. It is also necessary to define a system of axes, X_a, Y_a, Z_a, which is fixed to the antenna. In the absence of pitch, roll and yaw motions this system will coin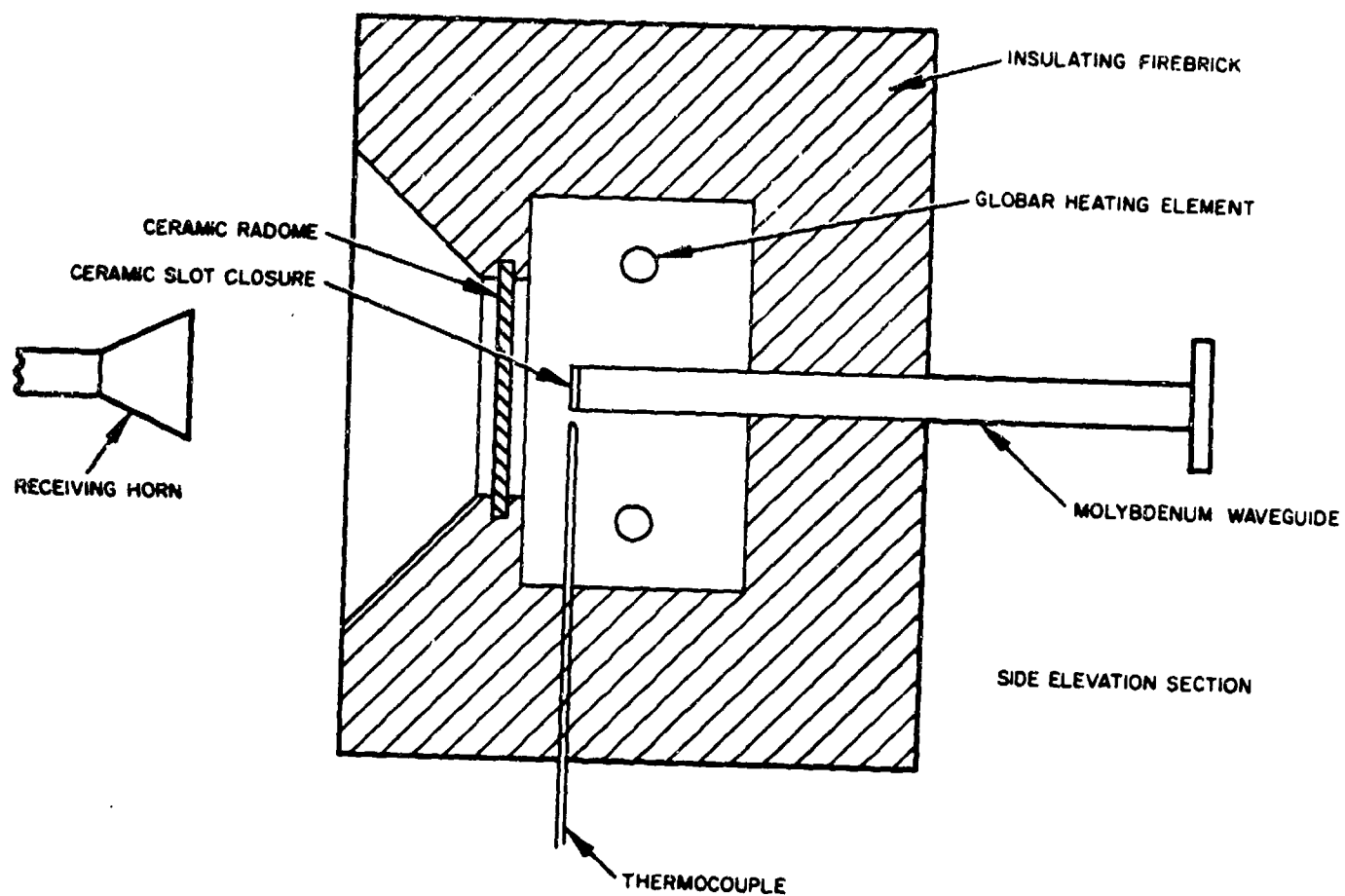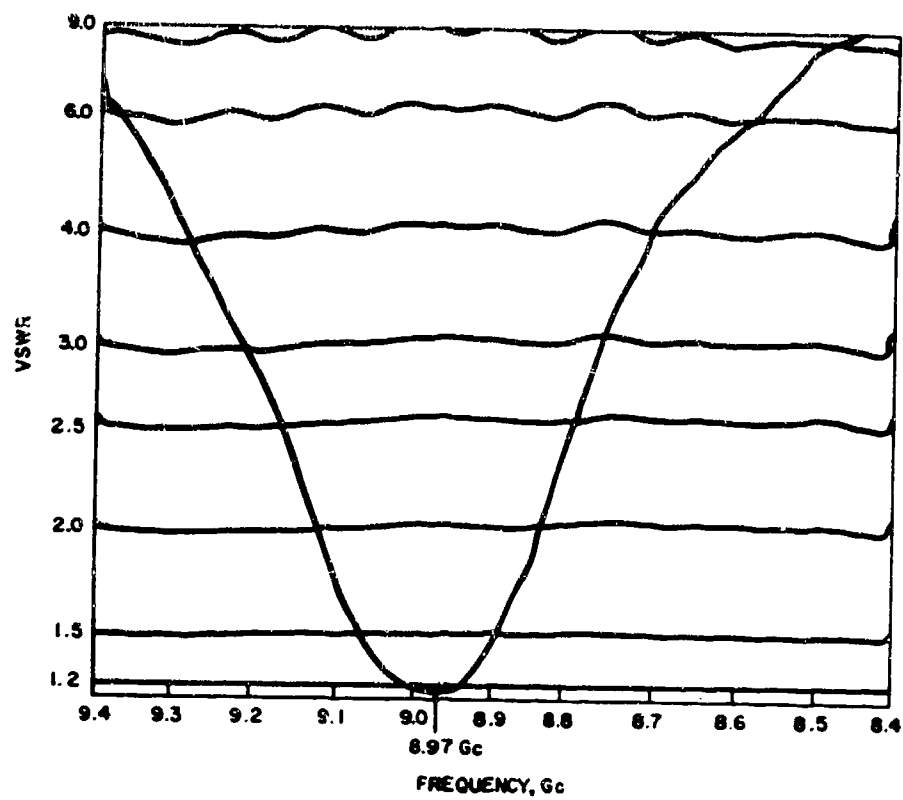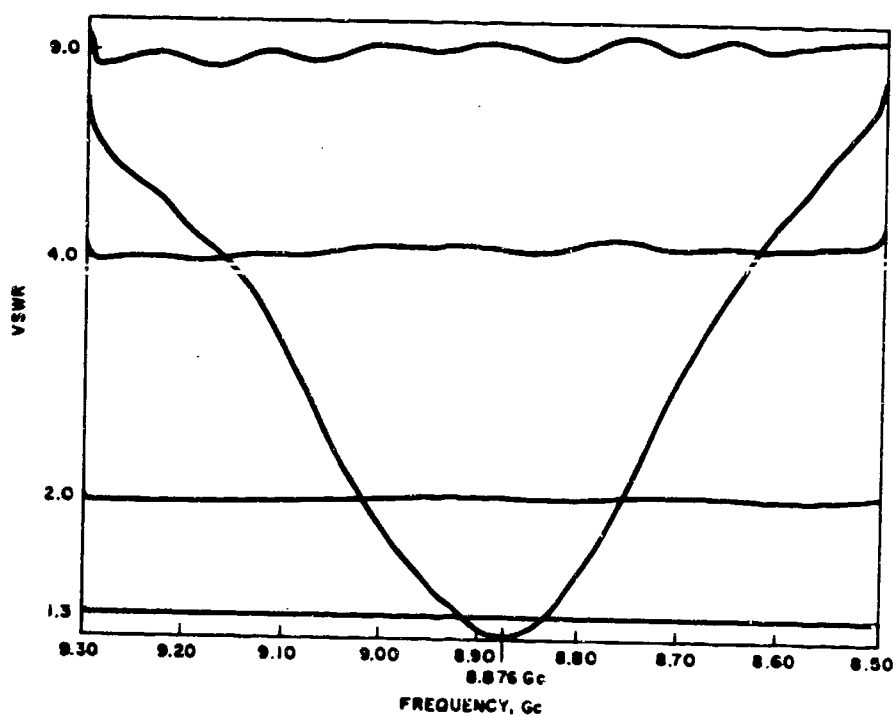cide with the reference axes. As the vehicle goes through various pitch, roll, and yaw angles the antenna axes rotate with respect to the reference axes.

We wish to relate a set of angles, θ_e and ϕ_e, fixed in the reference system, to their values θ_a and ϕ_a in the antenna coordinate system. The angles θ and ϕ are the usual spherical coordinates. The arrangement is illustrated in Figure 15. To derive the desired relationship consider the pitch, roll and yaw maneuvers described in Figure 16. The primed axes in these figures represent the initial position of the antenna axes.

The transformations from the primed coordinates to the final coordinates in each case are given by $\begin{bmatrix} Y \end{bmatrix}$, $\begin{bmatrix} R \end{bmatrix}$ and $\begin{bmatrix} P \end{bmatrix}$, the yaw, roll and pitch matrices respectively. We have
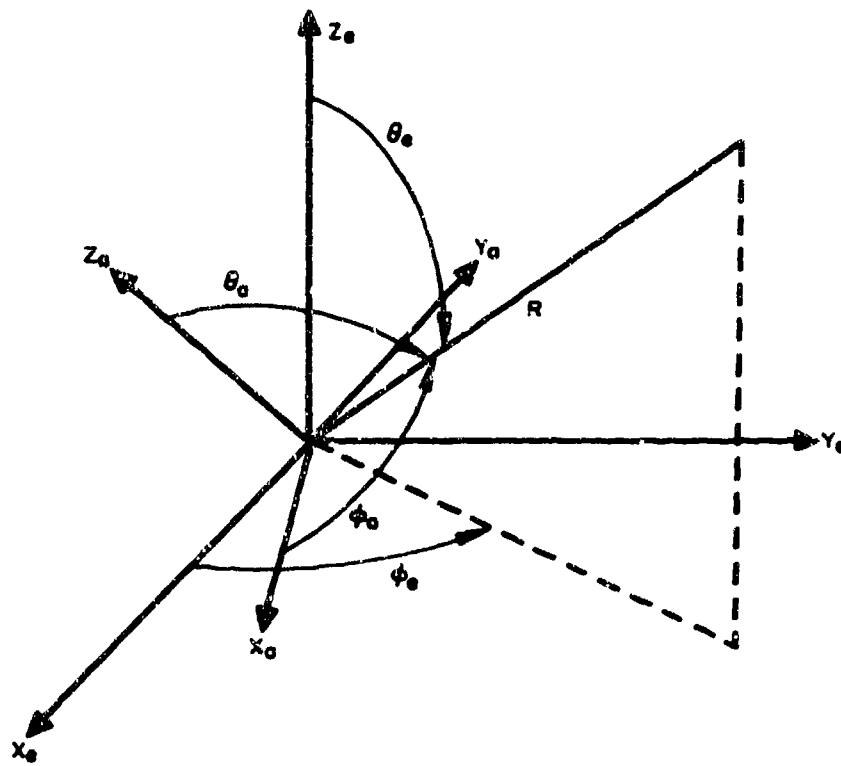
Figure 15. Rotated coordinate systems.

$$[Y] = \begin{bmatrix} \cos y & -\sin y & 0 \\ \sin y & \cos y & 0 \\ 0 & 0 & 1 \end{bmatrix}$$

$$[R] = \begin{bmatrix} \cos r & 0 & -\sin r \\ 0 & 1 & 0 \\ \sin r & 0 & \cos r \end{bmatrix}$$

$$[P] = \begin{bmatrix} 1 & 0 & 0 \\ 0 & \cos p & -\sin p \\ 0 & \sin p & \cos p \end{bmatrix}$$

36
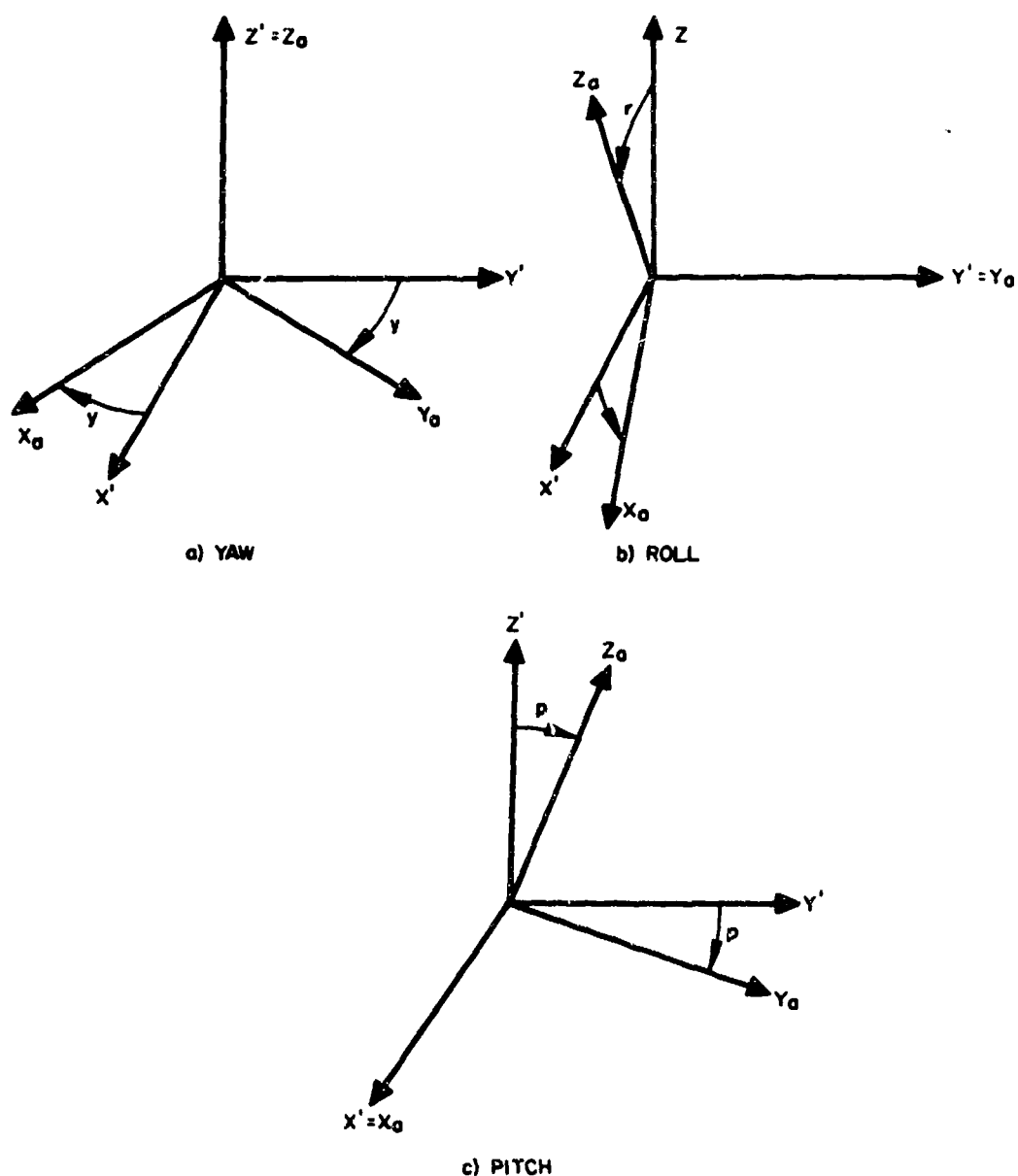
Figure 16. Definition of pitch roll and yaw.

The matrix $\begin{bmatrix} A \end{bmatrix}$ which describes the resultant orientation of the axes is the product of these three matrices. The value of this product, i. e. , the resulting position of the axes, depends on the order in which the maneuvers occur.

There are six possible combinations in which these may be taken. These combinations are as shown on the following page.

37

$$\begin{bmatrix}R\end{bmatrix} \quad \begin{bmatrix}P\end{bmatrix} \quad \begin{bmatrix}Y\end{bmatrix}$$

$$\begin{bmatrix}Y\end{bmatrix} \quad \begin{bmatrix}R\end{bmatrix} \quad \begin{bmatrix}P\end{bmatrix}$$

$$\begin{bmatrix}P\end{bmatrix} \quad \begin{bmatrix}Y\end{bmatrix} \quad \begin{bmatrix}R\end{bmatrix}$$

$$\begin{bmatrix}R\end{bmatrix} \quad \begin{bmatrix}Y\end{bmatrix} \quad \begin{bmatrix}P\end{bmatrix}$$

$$\begin{bmatrix}P\end{bmatrix} \quad \begin{bmatrix}R\end{bmatrix} \quad \begin{bmatrix}Y\end{bmatrix}$$

$$\begin{bmatrix}Y\end{bmatrix} \quad \begin{bmatrix}P\end{bmatrix} \quad \begin{bmatrix}R\end{bmatrix}$$

When these are carried out one gets

$$[Y][R][P] = \begin{bmatrix} \cos y \cos r & -\sin y \cos p - \cos y \sin r \sin p & \sin y \sin p - \cos y \sin r \cos p \\ \sin y \cos r & \cos y \cos p - \sin y \sin r \sin p & -\cos y \sin p - \sin y \sin r \cos p \\ \sin r & \cos r \sin p & \cos r \cos p \end{bmatrix}$$

$$[P][Y][R] = \begin{bmatrix} \cos y \cos r & -\sin y & -\cos y \sin r \\ \cos p \sin y \cos r - \sin p \sin r & \cos p \cos y & -\cos p \sin r \sin y - \sin p \cos r \\ \sin p \sin y \cos r + \cos p \sin r & \sin p \cos y & -\sin p \sin r \sin y + \cos p \cos r \end{bmatrix}$$

$$[R][P][Y] = \begin{bmatrix} \cos r \cos y - \sin r \sin p \sin y & -\cos r \sin y - \sin r \sin p \cos y & -\sin r \cos p \\ \cos p \sin y & \cos p \cos y & -\sin p \\ \sin r \cos y + \cos r \sin p \sin y & -\sin r \sin y + \cos r \sin p \cos y & \cos r \cos p \end{bmatrix}$$

$$[Y][P][R] = \begin{bmatrix} \cos y \cos r + \sin y \sin p \sin r & -\sin y \cos p & -\cos y \sin r + \sin y \sin p \cos r \\ \sin y \cos r - \cos y \sin p \sin r & \cos y \cos p & -\sin y \sin r - \cos y \sin p \cos r \\ \cos p \sin r & \sin p & \cos p \cos r \end{bmatrix}$$

$$[R][Y][P] = \begin{bmatrix} \cos r \cos y & -\cos r \sin y \cos p - \sin r \sin p & \cos r \sin y \sin p - \sin r \cos p \\ \sin y & \cos y \cos p & -\cos y \sin p \\ \sin r \cos y & -\sin r \sin y \cos p + \cos r \sin p & \sin r \sin y \sin p + \cos r \cos p \end{bmatrix}$$

$$[P][R][Y] = \begin{bmatrix} \cos r \cos y & -\cos r \sin y & -\sin r \\ -\sin p \sin r \cos y + \cos p \sin y & \sin p \sin r \sin y + \cos p \cos y & -\sin p \cos r \\ \cos p \sin r \cos y + \sin p \sin y & -\cos p \sin r \sin y + \sin p \cos y & \cos p \cos r \end{bmatrix}$$

As specified in the requirements of contract AF 33(616)-10672, the desired position of the beams with respect to the earth-reference axes is $\theta_e = 20°$, $\phi_e = 70°$ and $\theta_e = 20°$, $\phi_e = 290°$. Therefore,

$$\sin \theta_e \cos \phi_e \equiv u_e = 0.117$$

$$\sin \theta_e \sin \phi_e \equiv v_e = \pm 0.321$$

$$\cos \theta_e \equiv \sqrt{1 - u_e^2 - v_e^2} = 0.940$$

The upper sign corresponds to the forward looking beam, the lower sign to the backward looking beam. The coordinates of the beam relative to the antenna axes are given by six sets of relations as follows:

$$\begin{cases} \sin \theta_a \cos \phi_a = 0.117 \cos y \cos r \pm 0.321 \left[-\sin y \cos p - \cos y \sin r \sin p\right] -0.940 \left[-\sin y \sin p + \cos y \sin r \cos p\right] \\ \sin \theta_a \sin \phi_a = 0.117 \sin y \cos r \pm 0.321 \left[\cos y \cos p - \sin y \sin r \sin p\right] +0.940 \left[-\cos y \sin p - \sin y \sin r \cos p\right] \\ \cos \theta_a = 0.117 \sin r \qquad \pm 0.321 \cos r \sin p \qquad +0.940 \cos r \cos p \end{cases}$$

$$\begin{cases} \sin \theta_a \cos \phi_a = 0.117 \cos y \cos r \mp 0.321 \sin y \qquad -0.940 \cos y \sin r \\ \sin \theta_a \sin \phi_a = -0.117 \left[-\cos p \sin y \cos r + \sin p \sin r\right] \pm 0.321 \cos p \cos y +0.940 \left[-\cos p \sin r \sin y - \sin p \cos r\right] \\ \cos \theta_a = 0.117 \left[\sin p \sin y \cos r + \cos p \sin r\right] \pm 0.321 \sin p \cos y +0.940 \left[-\sin p \sin r \sin y + \cos p \cos r\right] \end{cases}$$

$$\begin{cases} \sin \theta_a \cos \phi_a = 0.117 \left[\cos r \cos y - \sin r \sin p \sin y\right] \pm 0.321 \left[-\cos r \sin y - \sin r \sin p \cos y\right] -0.940 \sin r \cos p \\ \sin \theta_a \sin \phi_a = 0.117 \cos p \sin y \pm 0.321 \cos p \cos y -0.940 \sin p \\ \cos \theta_a = 0.117 \left[\sin r \cos y + \cos r \sin p \sin y\right] \pm 0.321 \left[-\sin r \sin y + \cos r \sin p \cos y\right] +0.940 \cos r \cos p \end{cases}$$

$$\begin{cases} \sin \theta_a \cos \phi_a = 0.117 \left[\cos y \cos r + \sin y \sin p \sin r\right] \mp 0.321 \sin y \cos p -0.940 \left[\cos y \sin r - \sin y \sin p \cos r\right] \\ \sin \theta_a \sin \phi_a = -0.117 \left[-\sin y \cos r + \cos y \sin p \sin r\right] \pm 0.321 \cos y \cos p +0.940 \left[-\sin y \sin r - \cos y \sin p \cos r\right] \\ \cos \theta_a = 0.117 \cos p \sin r \qquad \pm 0.321 \sin p \qquad +0.940 \cos p \cos r \end{cases}$$

$$\begin{cases} \sin \theta_a \cos \phi_a = 0.117 \cos r \cos y \pm 0.321 \left[-\cos r \sin y \cos p - \sin r \sin p\right] -0.940 \left[-\cos r \sin y \sin p + \sin r \cos p\right] \\ \sin \theta_a \sin \phi_a = 0.117 \sin y \pm 0.321 \cos y \cos p \qquad -0.940 \cos y \sin p \\ \cos \theta_a = 0.117 \sin r \cos y \pm 0.321 \left[-\sin r \sin y \cos p + \cos r \sin p\right] +0.940 \left[\sin r \sin y \sin p + \cos r \cos p\right] \end{cases}$$

$$\begin{cases} \sin \theta_a \cos \phi_a = 0.117 \cos r \cos y \mp 0.321 \cos r \sin y \qquad -0.940 \sin r \\ \sin \theta_a \sin \phi_a = -0.117 \left[\sin p \sin r \cos y + \cos p \sin y\right] \pm 0.321 \left[\sin p \sin r \sin y + \cos p \cos y\right] -0.940 \sin p \cos r \\ \cos \theta_a = 0.117 \left[\cos p \sin r \cos y + \sin p \sin y\right] \pm 0.321 \left[-\cos p \sin r \sin y + \sin p \cos y\right] +0.940 \cos p \cos r \end{cases}$$

As specified in the Doppler contract, AF 33(616)-10672, pitch angles of from 10° to 30° (up) and roll angles of ±20° have been considered. Yaw angles have been neglected in the computations.

The required positions of the forward looking and backward looking beams, with respect to the antenna axes, have been computed for several combinations of pitch and roll. In order to maintain the beams in angular positions which are fixed relative to the earth oriented axes, X_e, Y_e, Z_e, it is therefore necessary to be able to scan the beam within certain areas with respect to th antenna axes. Several such areas are illustrated in Figures 17 through 20.

In Figures 17 and 18 it has been assumed that the vehicle rolls first and then pitches. In Figures 19 and 20 it has been assumed that it pitches first and then rolls. For the angles considered, the regions are quite similar and essentially overlap. The areas of required beam pointing positions are determined by the sum of these areas (once again neglecting yaw). The required pointing directions of the other forward and backward looking beams lie in areas which are the mirror images of these areas reflected across the v axis.

In the following sections techniques for positioning the beams are considered. These are then applied to a particular array to determine what beam positions may be obtained
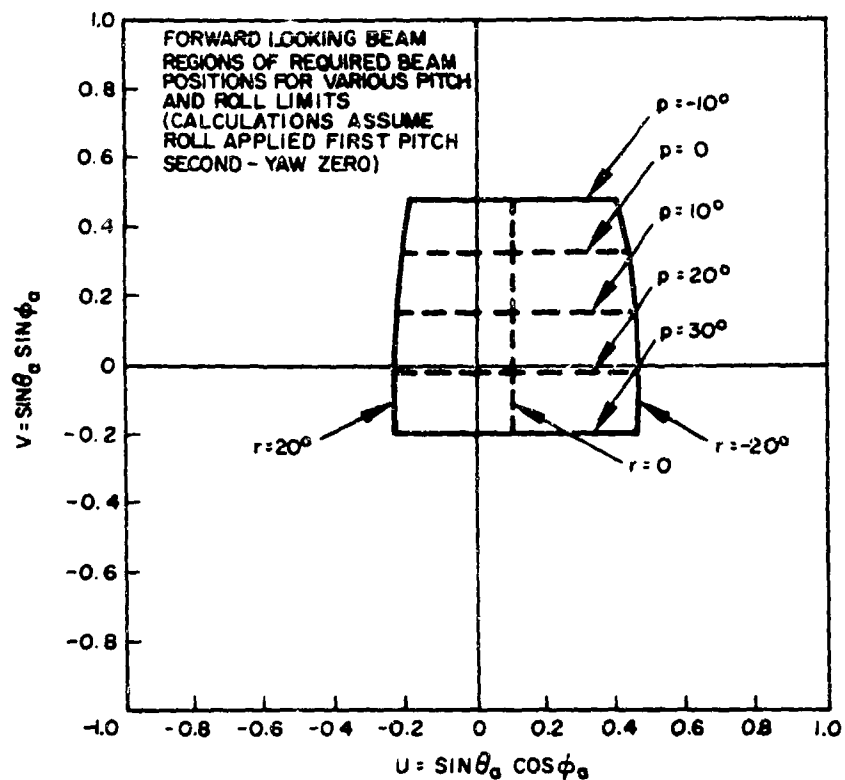
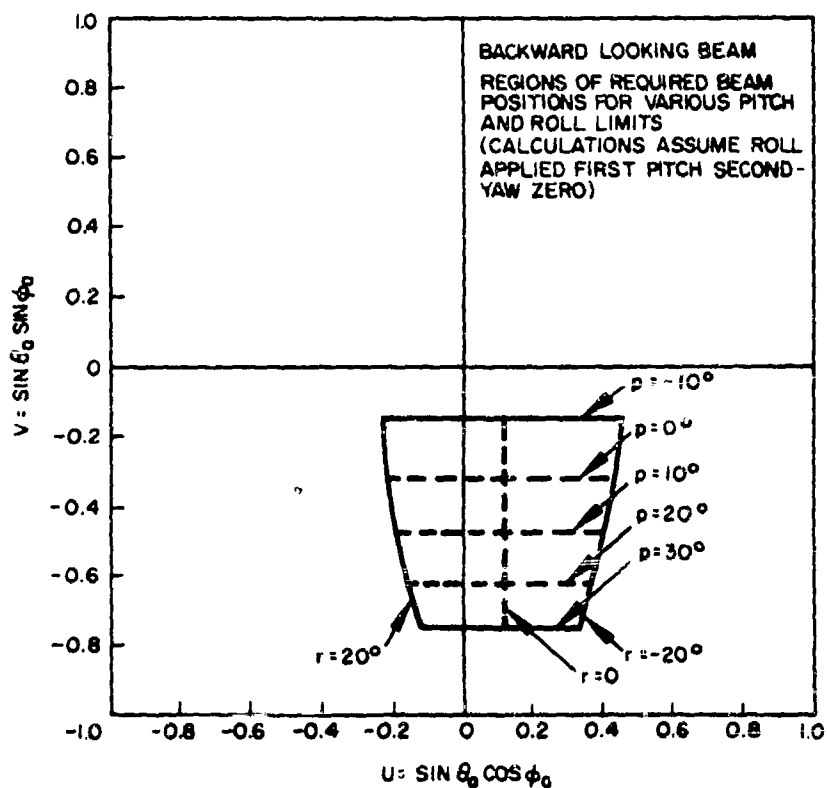Figure 17. Regions of required beam positions.
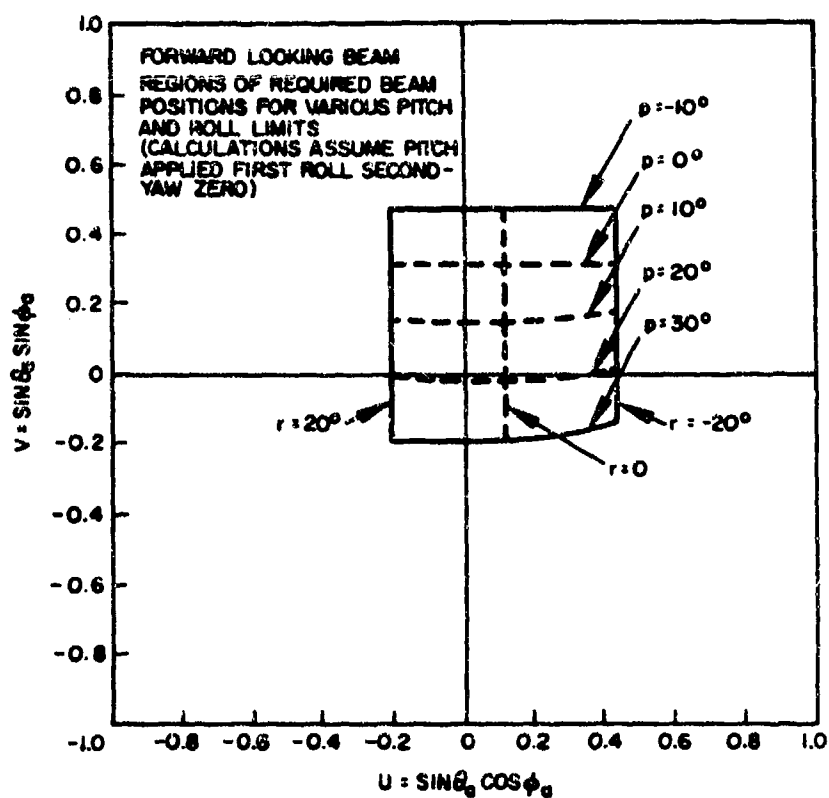

Figure 18. Regions of required beam positions.
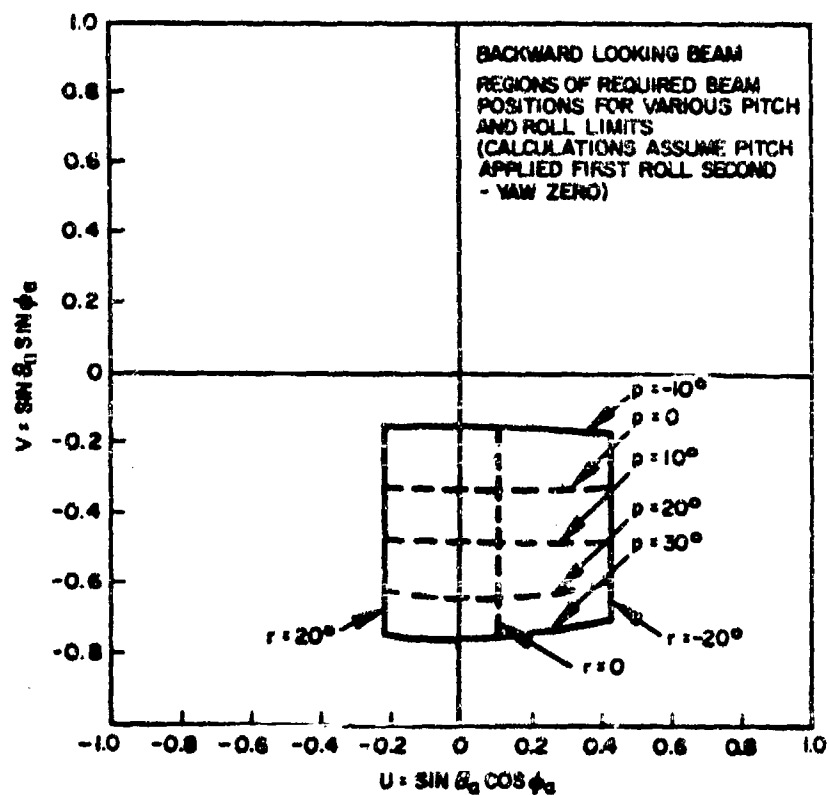
41

Figure 19. Regions of required beam positions.

Figure 20. Regions of required beam positions.

METHODS OF BEAM POSITIONING

In order to position the beam of an antenna pattern in a desired
spatial direction it is necessary to establish a certain phase distribu-
tion over the antenna aperture. This distribution must be such that
radiation from all radiating elements in the aperture arrive in phase
at a point located in the desired direction. A number of techniques
exist which can, in theory at least, accomplish this task. These usu-
ally employ one type or other of variable phase shifter interconnected
among the array elements in a manner which will depend upon the array
configuration, the power handling requirements, and on the frequency
range of interest. The actual type of phase shifter used will also depend
on these factors as well as on environmental conditions. This latter
consideration may well become the deciding factor in selecting the embod-
iment of the phase shifting technique. For the case of a high tempera-
ture environment the use of ferrite or diode phase shifters directly within
the waveguide does not appear feasible since neither are capable of with-
standing temperatures of 2500°F. Some other technique must be used
if the phase shifting is to be done at the elevated temperatures. For
example, it appears that a high temperature dielectric slab properly
inserted along a waveguide could be used as a variable phase shifter at
elevated temperatures. Such a device will be discussed in more detail
subsequently. Changes in frequency may also be used to produce effec-
tive interelement phase shift and thereby obtain beam scanning.

A combination of the techniques of using interelement phase
shifters and frequency variation (frequency scan) has therefore been
selected as a possibility for the flat plate type array. These techniques
may be adapted to the doppler antenna being developed under contract
AF 33(616)-10672. It is assumed that the array will use frequency scan
in one plane and phase shift scan in the orthogonal plane. The following
section considers the range of achievable beam positions for the antenna.

STUDY OF ACHIEVABLE BEAM POSITIONS

In keeping with the above mentioned type of array, the one studied here is assumed to be composed of parallel linear arrays oriented parallel to y-axis and spaced at distances d_x in the x-y plane as shown in Figure 21.
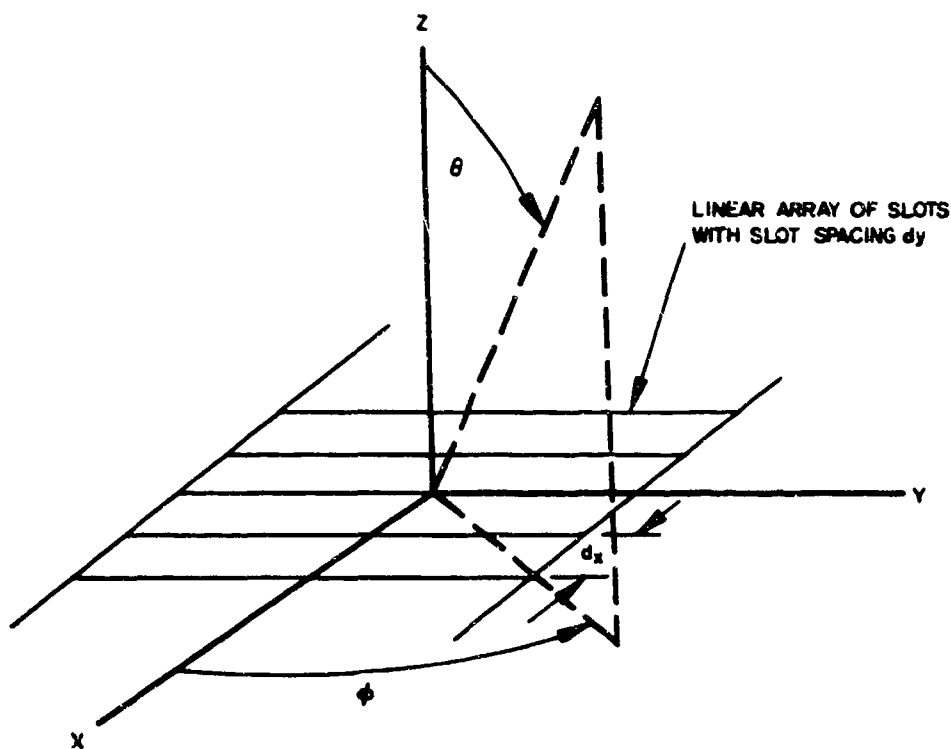
Figure 21. Two dimensional array orientation.

The radiating elements in the linear arrays are closely spaced slots so that the arrays are of the leaky wave type. The spacing between arrays, d_x, is determined by the width of the arrays. The frequency scan will be assumed in the y-z plane while the phase shift scan is assumed in the x-z plane.

Consider the plane in which only frequency scan exists. The array factor of the linear arrays will have maxima on cones with axes along the y-axis and defined by

$$\frac{2\pi}{\lambda} d_y \sin \theta_q \sin \phi_q - \frac{2\pi}{\lambda_y} d_y = 2\pi q \qquad q \text{ integer}$$

$$\text{i. e.} \qquad \sin \theta_q \sin \phi_q = q \frac{\lambda}{d_y} + \frac{\lambda}{\lambda_y}$$

To prevent multiple beams in visible space $\left| \sin \theta_q \sin \phi_q \right|$ must be greater than 1 for all values of q other than $q = 0$. This is satisfied if

$$d_y < \frac{\lambda_{min}}{1 + \lambda_{min}/\lambda_{ymin}} \equiv \frac{\lambda_{min}}{1 + \sqrt{1 - (\lambda_{min}/\lambda_{yc})^2}}$$

λ is the free space wavelength, λ_y is the guide wavelength in the y directed guides, λ_{yc} is the cutoff wavelength and the subscript "min" indicates the minimum wavelength of interest. The scan angle is now given by

$$\sin \theta_o \sin \phi_o = \frac{\lambda}{\lambda_y} = \sqrt{1 - (\frac{\lambda}{\lambda_{yc}})^2}$$

The cones are illustrated in Figure 22. The maximum cone half angle a_{max} occurs at the lowest frequency and is given by

$$\cos a_{max} = \frac{\lambda_{max}}{\lambda_{ymax}} = (\sin \theta_o \sin \phi_o)_{max} = \sqrt{1 - \left(\frac{\lambda_{max}}{\lambda_{yc}}\right)^2}$$
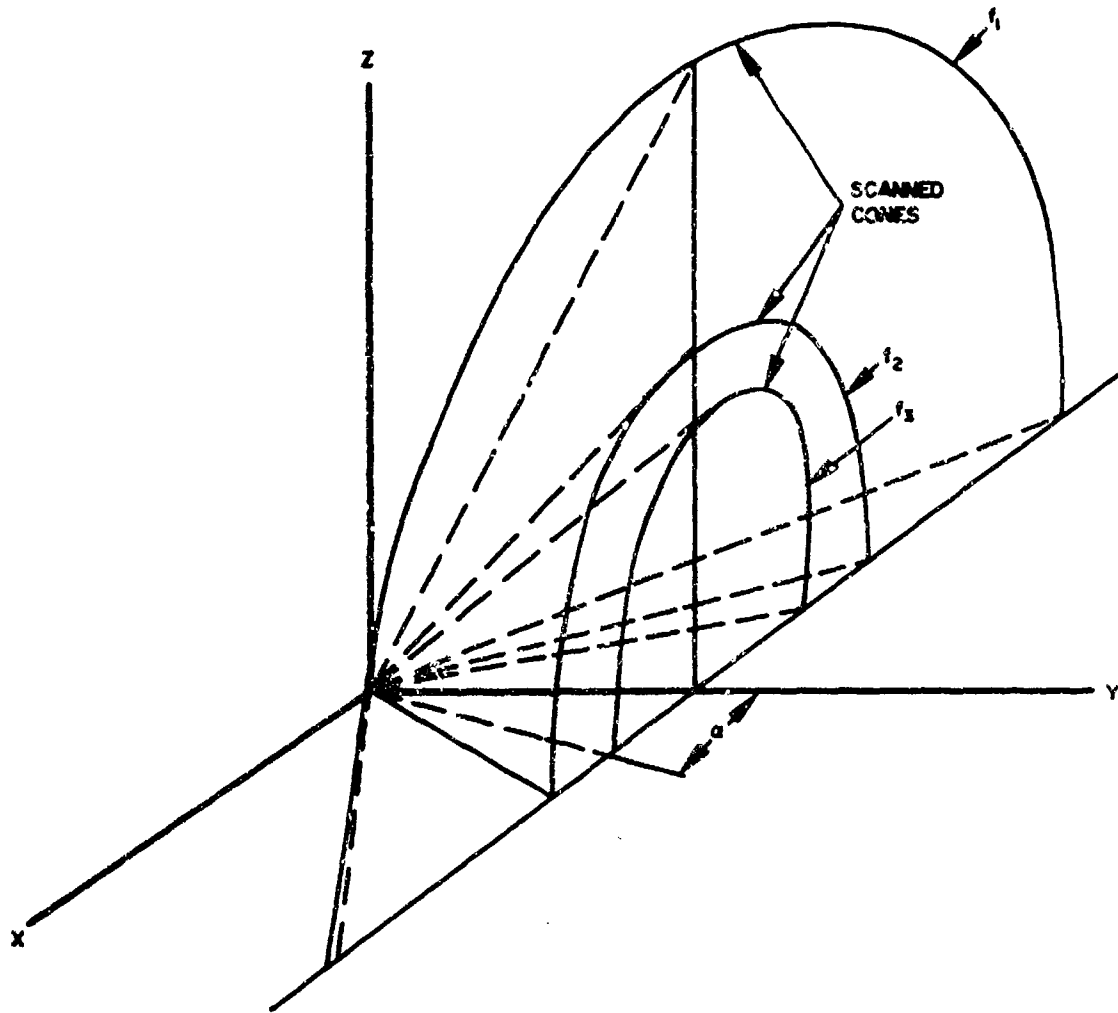
Figure 22. Frequency scanned cones $f_1 < f_2 < f_3$.

The minimum cone angle, α_{min} , occurs at the highest frequency and is given by

$$\cos \alpha_{min} = \frac{\lambda_{min}}{\lambda_{ymin}} = (\sin \theta_o \sin \phi_o)_{min} = \sqrt{1 - \left(\frac{\lambda_{min}}{\lambda_{yc}}\right)^2}$$

Consider next the array factor due to the combination of arrays parallel to the y-axis. This array factor will consist of beams which form cones with axes along the x-axis. The cones will scan with

interelement phase shift and with frequency. The phase shift, ψ can therefore be used to compensate for frequency scan in this plane. The cone angles are determined from

$$\frac{2\pi}{\lambda} \, d_x \sin \theta_p \cos \phi_p - \psi - 2\pi \frac{d_x}{\lambda_x} = 2\pi p \qquad p \text{ integer}$$

i.e. , $\quad \sin \theta_p \cos \phi_p = p \dfrac{\lambda}{d_x} + \sin \theta_o \cos \phi_o$

Once again, to avoid multiple cones in visible space we must have

$$\left| p \frac{\lambda}{d_x} + \sin \theta_o \cos \phi_o \right| > 1$$

for all p other than $p \cdot o$. This amounts to

$$d_x < \frac{\lambda_{min}}{1 + \left\lceil (\sin \theta_o \cos \phi_o)_{max} \right\rceil} = \frac{\lambda_{min}}{1 + \left\lceil \cos \beta_o \right\rceil_{max}}$$

where β_o is the half angle that the cones make with the positive x-axis. The phase shift, ψ , required to give a specified scan angle is now determined from

$$\frac{\lambda}{\lambda_x} + \frac{\lambda}{d_x} \frac{\psi}{2\pi} = \sin \theta_o \cos \phi_o$$

$$\frac{\psi}{2\pi} = \frac{d_x}{\lambda} \left(\sin \theta_o \cos \phi_o - \sqrt{1 - (\lambda/\lambda_{cx})^2} \right)$$

If we now write

$$d_x = \eta \frac{\lambda_{min}}{1 + \left| \sin \theta_o \cos \phi_o \right|_{max}}$$

where $0 < \eta < 1$ we get

$$\frac{\psi}{2\pi} = \eta \frac{\lambda_{min}}{\lambda} \frac{\left[\sin \theta_o \cos \phi_o - \sqrt{1 - \left(\frac{\lambda}{\lambda_{cx}} \right)^2} \right]}{\left[\left| (\sin \theta_o \cos \phi_o) \right|_{max} + 1 \right]}$$

There may be a restriction on the minimum allowable spacing $d_{x\ min}$. This may therefore limit the range of scan in $\sin \theta \cos \phi$. Otherwise, with sufficiently close spacing, i.e., $d < \lambda_{min}/2$ values of $\sin \theta_o \cos \phi_o$ from -1 to 1 may be obtained.

The total array factor is the product of the two array factors just considered. Therefore, beams occur only when the cones intersect and the actual restriction on the spacing d_x is not that multiple cones coaxial with the x-axis in visible space must be avoided, but that, if such cones exist, that they never intersect the cones which are coaxial with the y-axis. This requirement results in the restriction

$$\left| \cos \beta_o \right|_{max} < \frac{\lambda}{d_{..}} - \sin \alpha_{max}$$

Since the total array factor is the product of the two array factors considered, the beam pointing directions will therefore lie at the intersections of the cones as described above. At any particular frequency the resulting beam will scan along one of the fixed frequency cones as the interelement phase shift is varied.

As an example of the angles which can be covered consider the following example:

$$\text{guide width } \underline{a} = 0.80 \text{ inch}$$

$$\text{frequency } \underline{f}_{min} = 7.80 \text{ Gc.}$$

$$\underline{f}_{max} = 8.80 \text{ Gc.}$$

This gives:

$$\lambda_{max} = 1.512 \text{ inch}$$

$$\lambda_{ymax} = 4.63 \text{ inch}$$

$$\lambda_{max}/\lambda_{ymax} = 0.3271$$

$$\lambda_{min} = 1.341 \text{ inch}$$

$$\lambda_{ymin} = 2.458 \text{ inch}$$

$$\lambda_{min}/\lambda_{ymin} = 0.5455$$

Therefore as the frequency is changed from 7.8 Gc to 8.8 Gc the beam will move from a cone coaxial with the +y-axis and of half angle

$$\alpha_{max} = 70.9°$$

to one of half angle

$$\alpha_{min} = 57.0°$$

Also, because of the guide width of 0.80 inch the minimum separation, d_x, will be about 1.00 inch and the scan in the other plane will be restricted to a range of cone angles from 55.4° to 124.6° at the lowest frequency and from 63.3° to 116.7° at the highest frequency. The coverage region may best be illustrated in the u-v plane where

$$u = \sin \theta \cos \phi = \cos \beta$$
$$v = \sin \theta \sin \phi = \cos \alpha$$

This is the projection of the unit sphere onto a plane parallel to the array surface. This is shown in Figure 23.

Figure 23 shows the coverage region for a forward looking beam only. A beam designed to be backward looking would lie in a region which is the mirror image about the u-axis of the area shown in Figure 23.

On referring to Figures 17 through 20, it appears that if the antenna is flush mounted to a vehicle pitching from 10° to 30° the scanning techniques considered will not cover the required regions. However, if the antenna is mounted horizontally so that it pitches through angles from -10° to $+10^{\circ}$ as the vehicle pitches from 10° to 30° then most of the required region may be covered by the combination of frequency scan and phase shift scan.
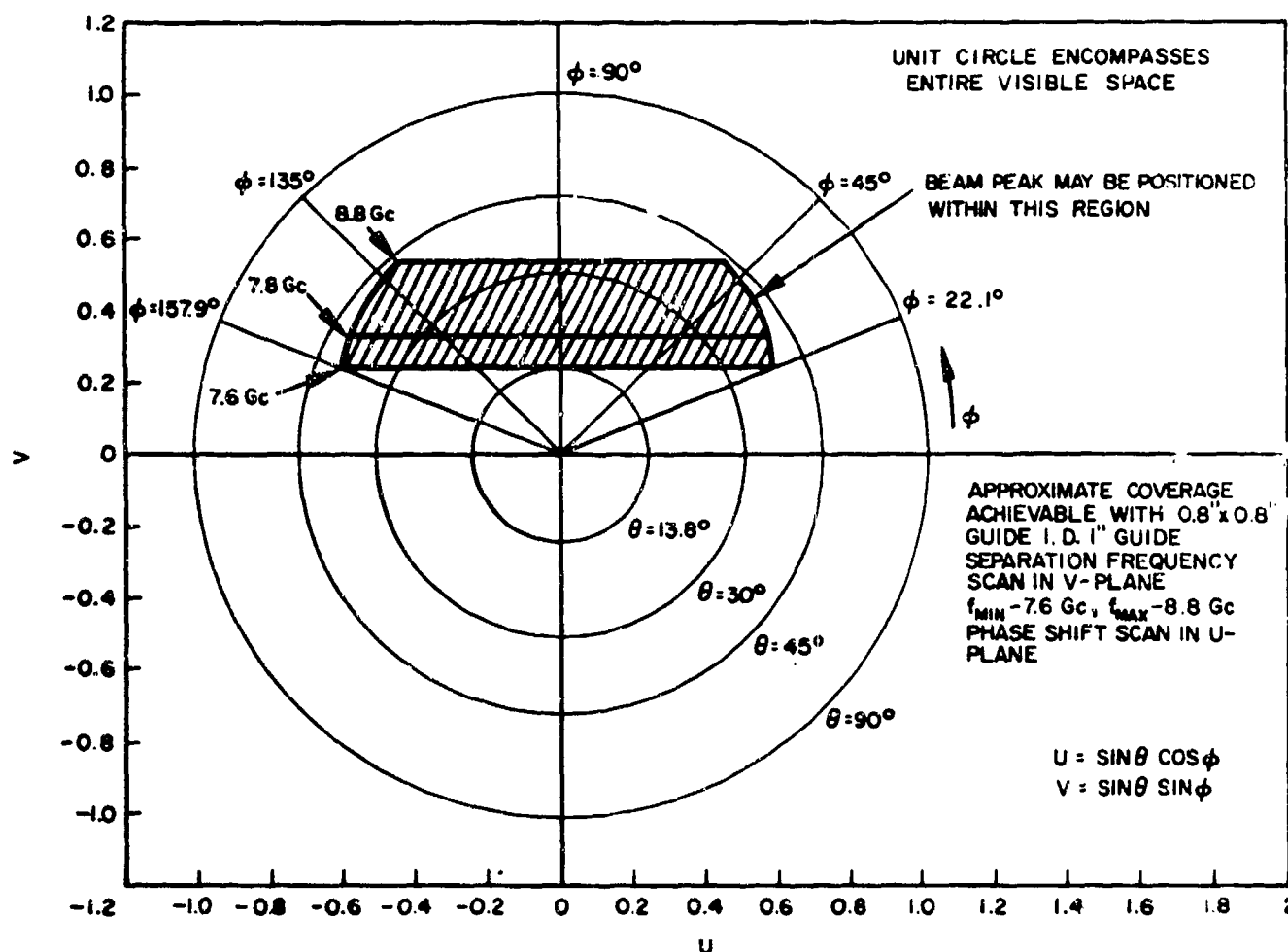

Figure 23. Approximate coverage achievable.

ELECTROMECHANICAL PHASE SHIFTING TECHNIQUE

In order to accomplish the phase shift beam scanning at high temperatures, as discussed in the previous section, it appears that an electromechanical technique would be desirable. As has already been mentioned, in the section on methods of beam positioning, the use of movable high temperature dielectric slabs in the guide appears desirable for the environmental conditions of interest in this study. Two configurations have been proposed for the doppler antenna. The general forms of these configurations are shown in Figures 24a and 24b. In Figure 24a, a square guide is used to carry the two orthogonal modes, TE_{10} and TE_{01}. One mode couples to the branch lines to form a beam in one direction while the second mode couples to the branch lines to form a beam in a second direction. The insertion of a single thin longitudinal dielectric slab into the guide along the centerline of one wall would affect the phase velocity of one mode without a major effect on the phase velocity of the other mode, and vice versa. With perfect geometry no mode coupling will take place. However, with both slabs present simultaneously it appears that mode coupling would become a problem. Therefore, the configuration of Figure 24b is more attractive. This eliminates the mode coupling problem in the feed guides by feeding the square branch guides from separate feed guides through orthogonal mode couplers.

The amount of differential phase shift obtainable with such dielectric slabs will depend on several factors. These are: (1) the dielectric constant of the slab, (2) the width of the slab, (3) the depth of insertion of the slab. The greater the dielectric constant of the slab material the greater the range of differential phase shift which will be obtainable. As an example of the differential phase shift per inch obtainable with a dielectic slab in going from zero insertion to full insertion, the differential phase shift in degrees per inch has been determined for several cases. The results are shown in Table 6. The guide width is a, the free space wavelength is λ, and the slab width is d. The calculations correspond to a = 0.800 inch and frequencies of 7.60 Gc, 7.80 Gc and

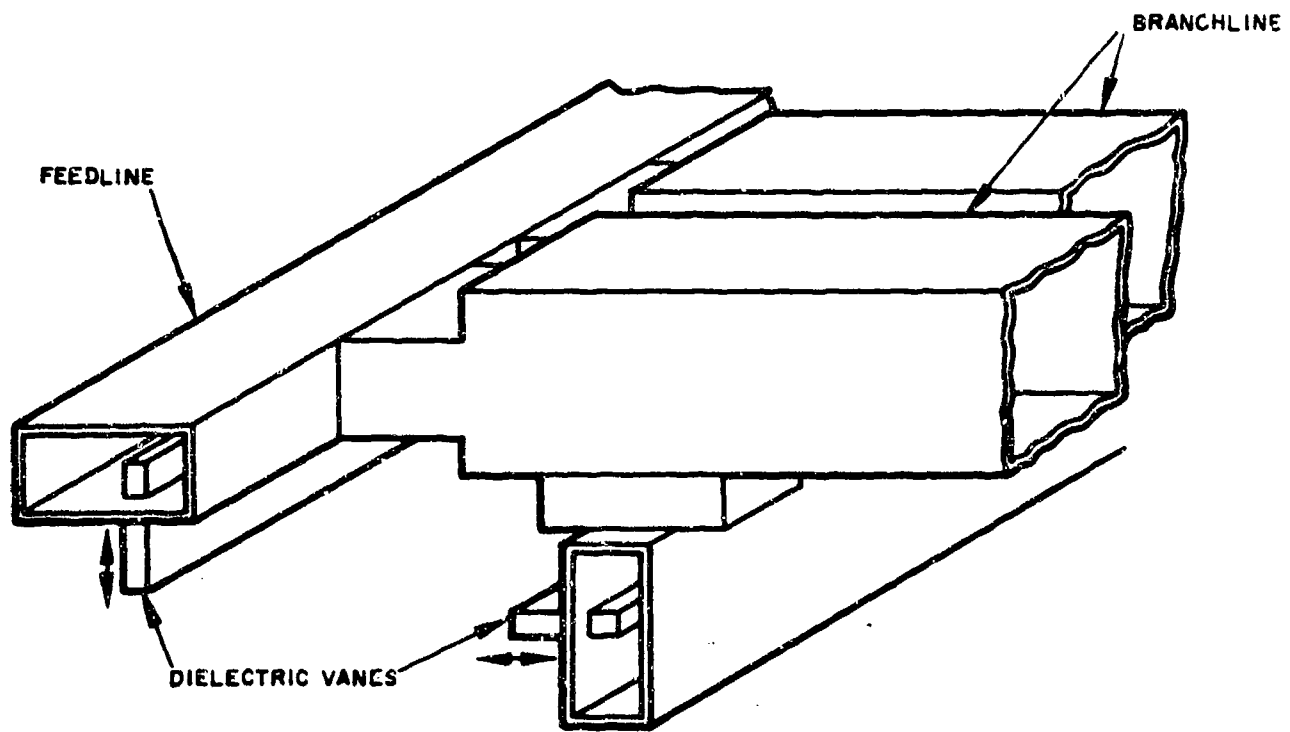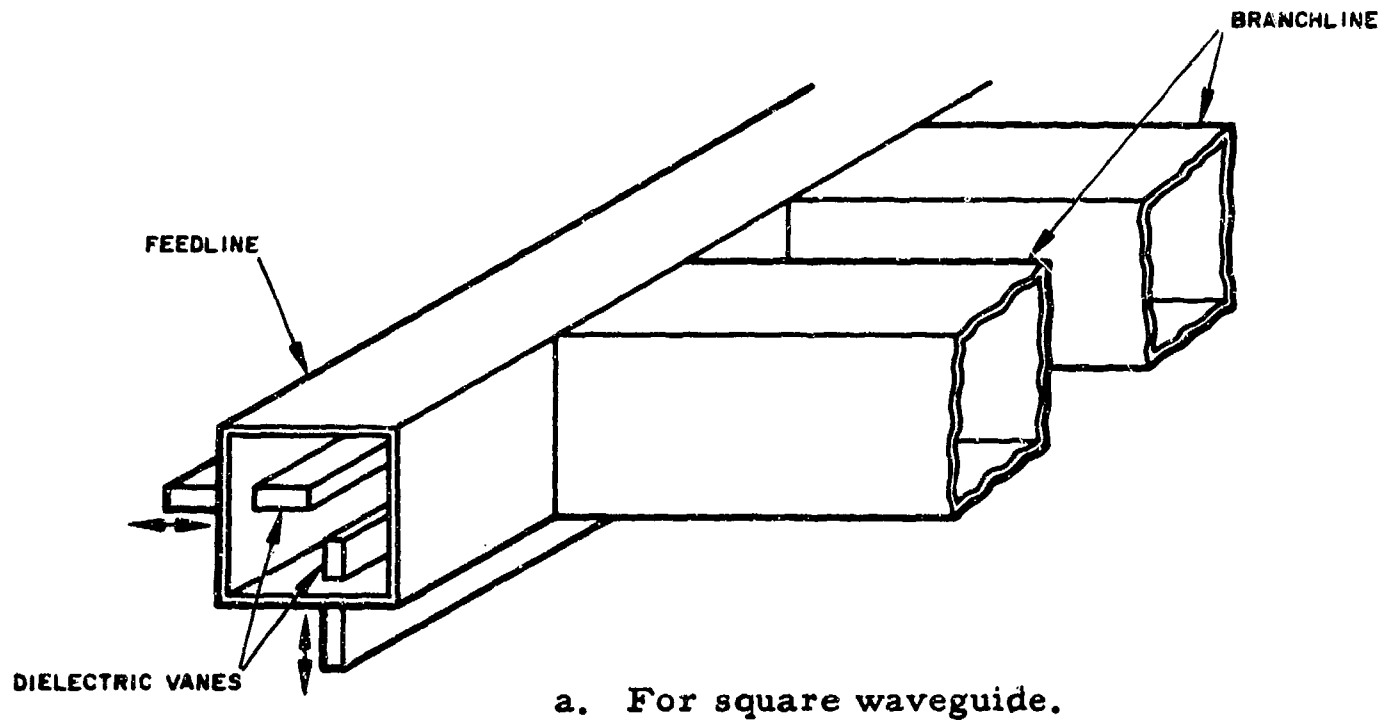BRANCHLINE

FEEDLINE

DIELECTRIC VANES

a. For square waveguide.

BRANCHLINE

FEEDLINE

DIELECTRIC VANES

b. For rectangular waveguide.

Figure 24.   Schematic of dielectric vane phase
shifter to be used in feed lines.

52

8.80 Lc. The value of relative permitivity, ϵ_r, is 2.45. This value was used because the phase shifts could be obtained from readily available sources.[5,6] The use of higher permitivity dielectric would increase the range of phase shifts obtainable.

a/λ \ d/a	0.10	0.20	0.30
0.515	82°/in.	131°/in.	165°/in.
0.529	76°/in.	123°/in.	158°/in.
0.596	61°/in.	111°/in.	143°/in.

Table 6. Maximum differential phase shift
using dielectric slab ($\epsilon_r = 2.45$)

There appears to be at least one difficulty with this proposed type of phase shifter, however. The use of wide slabs inserted into the guide may be accompanied by a tendency of the waves to couple out of the guide through the dielectric. This would require the use of a choking arrangement to prevent such coupling by presenting a virtual conducting wall coincident with the slot thereby making the broadwall appear continuous to the waves in the guide. This apparent difficulty may be obviated by replacing the dielectric slab with a conducting slab. Some choking would still probably be necessary but good effective contact

between the slab and the slot walls probably could be obtained. The configuration would be basically that of Figure 24b with the dielectric replaced by a movable metallic slab. Since the conducting slab has essentially an infinite dielectric constant one also might expect to obtain a wider range of differential phase shift from the metal slab than from a dielectric slab.

Table 7 shows the range of differential phase shift obtainable with a metallic slab[7] whose thickness is 0.05 of the guide width for various insertion depths, $\mathcal{L}/b$. The ratio of guide height to guide width is 0.45. It may be seen that at the higher frequency the differential phase shift for a slab extending into the gui as much as 80 percent of the guide height results in less phase shift than is obtained with the dielectric slab. Further insertion of the metal slab to produce additional phase shift would seriously reduce the guide impedance and might result in matching and coupling problems as the phase is varied. In addition, dissipation loss can be expected to increase significantly as the slab is inserted further. Based on these considerations it appears that even with the requirements for chokes mentioned above, the dielectric slab phase shifter may be preferable to the metallic slab phase shifter. Use of a sufficiently high dielectric constant material, e. g., alumina, would increase the maximum phase shift attainable over the values shown in Table 6. It must be pointed out, however, that the presence of the dielectric in the waveguide will also alter its impedance characteristics and will affect the coupling of energy from it to the branch guides. This should be further investigated to determine its effect on the performance of an array.

$a/_\lambda$ \ $\ell/_b$	0	0.20	0.35	0.50	0.65	0.75	0.80
0.515	0	33°/in.	67°/in.	94°/in.	118°/in.	131°/in.	138°/in.
0.596	0	15°/in.	35°/in.	54°/in.	71°/in.	85°/in.	89°/in.

Table 7. Differential phase shift versus depth of metal slab
(ratio of slab width to guide width = 0.05)
(ratio of guide height to width = 0.45)

CONCLUSIONS AND RECOMMENDATIONS

This report includes a study of two aspects of problems relating to the operation of flush-mounted slotted arrays on lift reentry vehicles. The first portion of the study dealt with the problem of slot closure techniques capable of withstanding temperatures of up to 2500°F. The second portion of the study dealt with the problem of beam stabilization during vehicle reentry maneuvers.

As a consequence of the first portion of the study the following conclusions may be reached:

1. Vacuum tight slot closures suitable for operation up to 2500°F have been developed.

2. Mullite ($3 Al_2O_3 - 2 SiO_2$) is the most promising ceramic window material for use with molybdenum.

3. Platinum, applied as thin foil interface, promotes exceptional adherence between mullite and molybdenum.

4. Alumina is unsuitable for use with molybdenum because of thermal expansion differential, and poor thermal shock resistance.

5. Ceramic waveguide with close dimensional tolerance appears feasible.

6. Molybdenum can be successfully coated with a high temperature glaze. The glaze can also be used to provide adherence between molybdenum, and mullite and zircon windows.

7. A test apparatus was designed for dielectric evaluation of slot closures to 2500°F.

8. Fabrication of molybdenum waveguides to the specified dimensional requirements by electron beam welding is feasible.

It is recommended that further investigations of the promising bonding and waveguide fabrication techniques be made so that reliable, repeatable radiating elements for large high temperature arrays may become available for future reentry vehicle applications. Such techniques are not necessarily limited to construction of array elements but should be useful in any situation where ceramics and refractory materials must be formed or bonded.

The study of beam stabilization requirements has shown that relatively few techniques appear readily adaptable to the scanning of the beam of high temperature arrays. Two techniques were, therefore, considered. These consisted of frequency scan in one plane and phase shift scan in the orthogonal plane. The phase shift scan technique considered was electromechanical, employing movable high temperature dielectric slabs in the feed guides to accomplish scanning.

The required beam scanning positions for the planar array were determined from typical pitch and roll angles for the antenna as specified in Contract AF 33(616)-10672. These were compared with achievable scan angles using the techniques of frequency scan and phase shift scan. It was found that if the antenna were normally oriented horizontally then most of the required beam pointing directions could be covered.

.

REFERENCES

1. W. F. Croswell and R. B. Higgins, NASA, Langley, Virginia, private communication.

2. "Introduction to Metals for Elevated-Temperature Use," Defense Metals Information Center Report 160, 27 October 1961, Battelle Memorial Institute.

3. A. Goldsmith et al., "Thermophysical Properties of Solid Materials," Armour Research Foundation, August 1960, WADC-TR-58-476, AD 247193.

4. S. D. Elrod and J. T. Stacy, "Fabrication of High Temperature Refractory Alloy Antennas," presented at AIME Conference on Applied Aspects of Refractory Metals, Los Angeles, 9 and 10 December 1963.

5. T. Moreno, "Microwave Transmission Design Data," Publication No. 23-80, Sperry Gyroscope Company, Inc., New York, New York, 1944; pp. 168-170.

6. A. D. Berk, "Variational Principles for Electromagnetic Resonators and Waveguides," IRE Transactions on Antennas and Propagation, Vol. AP-4, No. 2, April 1956, pp. 104-111.

7. Microwave Engineers' Handbook, Horizon House, Inc., 1964, p. 58.

AL TDR 64-162. DOPPLER ANTENNA INVESTIGATION. Unclassified.
Aerospace Group, Hughes Aircraft Company, Culver City, California.
Villeneuve, A. T. et al. C AF 04(695)-250. P 3181. T 318102. SRN P64-15.
In DDC. Aval frm OTS.

This report presents the results of a study dealing with the effects of
factors such as high temperature and vehicle maneuvers on a rectangular
flat plate slot array antenna for lift-reentry vehicles. Specifically, the
study consisted of two parts. The first part dealt with an investigation
of slot closure techniques which will preserve the electrical performance
of the antenna under severe environmental conditions. This consisted of
a materials study to determine suitable metals and dielectric materials
which have compatible thermodynamic characteristics up to temperatures
of $2500^{\circ}F$. When suitable materials had been determined, a number of
dielectric to metal bonding techniques were investigated experimentally.
The most successful of these bonding techniques was then investigated
to determine the electrical properties of the configuration. As a result
of the slot closure study several slots were fabricated in molybdenum
plates. These were closed with mullite and electron beam welded to the
end of a section of molybdenum X-band guide. The guide itself was
electron beam welded from sheet molybdenum. The guide and window
together showed insertion losses of 0.35 to 0.45 db at resonance when
tested under ambient temperature conditions. High temperature elec-
trical measurements were not performed in this phase of the program.
The second part of the study consisted of an investigation of the problem
of beam stabilization in the presence of vehicle pitch, roll, and yaw
maneuvers. Two aspects of the problem were considered. First, the
regions within which beam pointing control is required were determined
by applying various combinations of pitch and roll to the vehicle carrying
the antenna. Since it was anticipated that yaw would be small, it was
not considered in numerical calculations. Second, for the type of antenna

being considered, the region of possible beam positions was investigated. Devices and techniques for accomplishing the beam positioning were also considered. The high temperatures of the antenna and components ruled out the use of the most conventional phase shifting devices. The results of the beam stabilization studies indicate that for the types of stabilization considered for the flat plate antenna developed under Contract AF 33(616)-10672, the necessary beam positions cannot be obtained with a flush mounted array due to vehicle attitudes during reentry. However, if the array were set so as to be level when the vehicle had its normal attitude, then most of the desired angles could be covered.

RCS AFSC-R47